52. PALEOMAGNETISM OF DEEP SEA DRILLING PROJECT LEG 60 SEDIMENTS AND IGNEOUS ROCKS FROM THE MARIANA REGION[1]

Ulrich Bleil,[2] Institut für Geophysik, Ruhr-Universität, Bochum, Federal Republic of Germany

INTRODUCTION

As a typical example of an active back-arc basin, the Mariana Trough has attracted increasing attention in recent years. Intensive surface-ship geophysical observations, including the IPOD site survey along the south Philippine Sea transect, have resulted in a complex picture of a marginal basin with current crustal extension above a Benioff zone (Karig et al., 1978). Several lines of evidence indicate that the major zone of crustal accretion is confined to a central topographic high about halfway between the scarp systems bounding the trough, and that spreading was roughly symmetric (Karig, 1971). Estimates of spreading rate on the basis of geologic data for the widest area of the Mariana Trough, at 18°N, range from more than 6 cm/y. (Karig and Glassley, 1970) to 8–10 cm/y. (Karig, 1975).

It is difficult to specify the mode of opening in many marginal basins because of rather poorly defined patterns of lineated magnetic anomalies, which may result from a diffuse magma injection (Lawver and Hawkins, 1978). In general, the magnetic anomalies in the Mariana Trough cannot be correlated even over short distances, and a well-defined central anomaly is not observed in most available profiles. However, in the part of the basin that has been surveyed in greatest detail, near 18°N, Bibee and Shor (1978) identified a pattern of anomalies symmetric about the axial graben that are tentatively modeled by spreading at a (full) rate of 3 cm/y. for the past 3 m.y.

In this study, paleomagnetic results are reported for both sedimentary and igneous rock drill cores recovered at four sites in the Mariana Trough and another two sites in the Mariana fore-arc region during DSDP Leg 60 (Table 1). The objectives of this paper are: (1) to discuss the paleomagnetic pattern obtained for the individual drill holes in terms of a recording of the earth's magnetic field history, paleolatitudes, local and regional tectonics; and (2) to document a paleomagnetic framework for the Mariana transect to further the geological understanding of the area, and in particular to establish constraints for the opening of the Mariana Trough.

Rock magnetic data and oxide mineralogy of igneous samples are reported elsewhere.

Table 1. Site information.

Hole	Location	Basement Age[a]	Drilling (m)[b] Cored	Drilling (m)[b] Recovered	Samples
453	17°54′N 143°41′E	Oldest Pliocene	455.5/149.5	203.5/33.3	34/22
454A	18°01′N 144°32′E	Early Pleistocene	38.0/104.5	21.0/20.0	–/24[c]
456	17°55′N 145°11′E	Early Pleistocene	134.5/34.5	28.6/3.7	8/4
456A	17°55′N 145°11′E	Early Pleistocene	95.0/45.0	35.4/2.3	12/–
458	17°52′N 146°56′E	Early Oligocene	256.5/209.0	133.6/35.8	6/39
459B	17°52′N 147°18′E	Middle Eocene	558.9/132.6	158.6/23.5	110/26

[a] Based on age of overlying sediments, using an adapted Bukry (1975) nannofossil time scale (see paleontologic chapters, this volume).
[b] The first number refers to sediments, the second to basement rocks.
[c] Including interbedded sediments.

EXPERIMENTAL PROCEDURES

Approximately 10-cm^3 minicore samples were taken from the working half of the split main core. Sampling and orientation techniques used are those described by Ade-Hall and Johnson (1976). In the sediments, areas indicating features of a horizontal bedding were preferentially sampled. Directions and intensities of natural remanent magnetization (NRM) were measured with a Digico spinner magnetometer both aboard ship and at the University of Münster, Germany. Initial susceptibility measurements were made using a calibrated commercial suspectibility bridge (Bison Model 3101A). Shipboard and shorebased alternating field (AF) demagneti zation was performed on a Schonstedt GSD-1 single-axis demagnetizer. Systematic stepwise AF demagnetization was carried out to about 10 percent of the initial magnetization intensity and at least up to 500 Oe. The stable remanent magnetization direction for each sample has been defined by means of vector diagram plots (Zijderveld, 1968). The values given in the tables (see Appendix) are means over several consecutive demagnetization steps yielding a minimum of directional variation. Whenever the standard deviation (s.d.) exceeded 5°, the stable inclination and/or declination values listed are bracketed; no results are indicated for s.d. >10°.

Owing to the limited sensitivity of the equipment available, most attempts to isolate satisfactory paleomagnetic information failed for samples with an initial

[1] *Initial Reports of the Deep Sea Drilling Project*, Volume 60.
[2] Present address: Department of Geological Sciences, University of California, Santa Barbara, California.

magnetization intensity of less than 10^{-6} emu/cm³. Several igneous samples recovered at Site 453 were thermally demagnetized up to 600°C, using a Schonstedt TSD-1 device.

A mean ambient Earth's magnetic field intensity of F = 0.37 Oe as measured during Leg 60 at the various drill sites was used to calculate the Königsberger ratios.

RESULTS

The paleomagnetic data are given on a sample-by-sample basis in the Appendix. The tables include intensity (J_{NRM}), inclination (I_{NRM}), and declination (D_{NRM}) of natural remanent magnetization and stable remanent directions (I_{stable}, D_{stable}) at an optimum demagnetization stage. Although the actual declination is arbitrary as only the sense of the vertical axis is known for the drill cores, the relative change for each sample illustrates its magnetization stability. For the igneous samples analyzed, additionally the median destructive field (MDF), the alternating field necessary to reduce J_{NRM} to 50 per cent, the initial susceptibility (k), and the Königsberger ratio ($Q = J_{NRM}/kF$) are listed.

Site 453

This site is situated near the scarp of the West Mariana Ridge (remnant arc) marking the western boundary of the Mariana Trough (Figure 1). Paleomagnetic measurements were made on 34 samples from the Pliocene sedimentary sequence overlying the uppermost igneous rock layer recovered at this site. Widely divergent natural remanent intensities were encountered, spanning the range from less than 10^{-8} emu/cm³ to about 7×10^{-4} emu/cm³ (arithmetic mean: 73.5×10^{-6} emu/cm³). The highest intensities were measured in various volcanic ash layers. The lowest intensities were found in claystones and mudstones between about 270 and 295 meters below the sea floor, and in sandstone samples near the base of the sedimentary section at about 440 meters sub-bottom. Most samples with $J_{NRM} > 10^{-6}$ emu/cm³ revealed considerable magnetic stability upon partial AF demagnetization, median destructive fields typically ranging from 200 to 400 Oe. Generally, only minor directional changes were observed between the initial NRM stage and the final stable direction, indicating the presence of mostly rather small spurious magnetization components.

The variation of magnetic inclination with depth in the lower sediment layer is shown in Figure 2A. A pattern of consecutive sections of positive and negative magnetization directions is evident. In order to link this sequence of magnetic polarities to a geomagnetic polarity time scale, the following paleontological information (see paleontologic chapters, this volume) was used: (1) the 3-m.y. boundary (*Discoaster tamalis/Discoaster asymmetricus*) occurs at a sub-bottom depth of about 170 meters and (2) there is no indication of Miocene (Messinian) species in the lowest sediments. On the basis of these calibrations, the present data closely fit established Earth's magnetic field chronologies for parts of the Gauss normal and Gilbert reversed epoch. The latter comprises four distinct normal polarity intervals

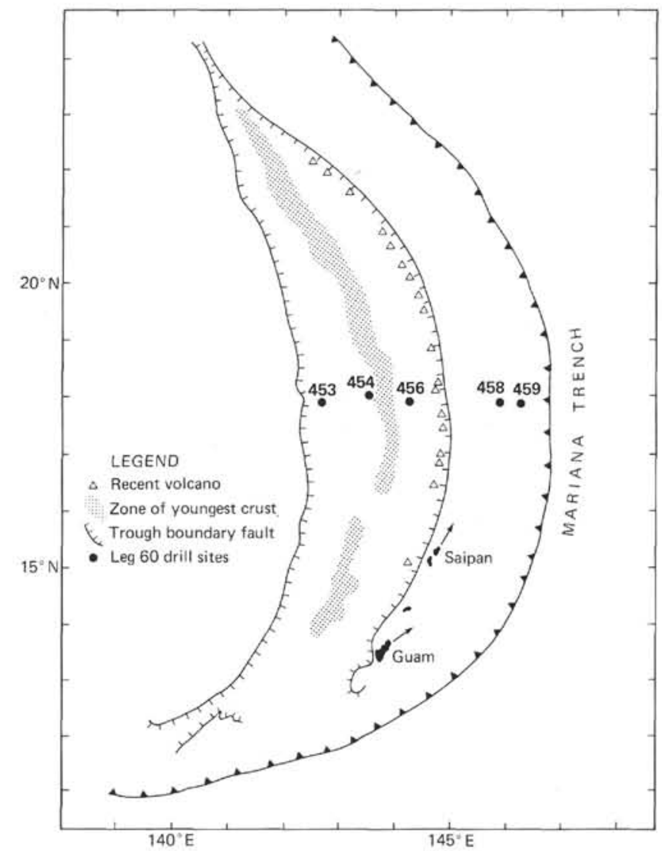

Figure 1. Sketch map of the Mariana Trough and fore-arc region, showing DSDP Leg 60 drilling site locations and outlines of the general geological setting (after Karig et al., 1978). Arrows at islands indicate amount of rotation since Miocene (see text for details).

(events), which all were tentatively identified here (see Fig. 2A for details). Using the geomagnetic polarity time scales of LaBreque et al. (1977) and McDougall (1977), respectively, the accumulation rate derived from the magnetic polarity log of the lower sedimentary sequence in this hole is in fair agreement with the paleontological data. For most of the interval, however, the magnetic ages are consistently younger than those indicated by calcareous nannofossils. Provided this is not because of a systematic discrepancy between the different time scales used, a possible explanation would be that the ridges surrounding the basin drilled acted as an immediate source for the sediment which accumulated on these ridges and was later mobilized into the basin. A somewhat puzzling feature is the anomalously shallow inclinations observed in the sediments as compared with the actual latitude of the site (see Table 2). This will be discussed more fully in a later section.

Extrapolation of the sediment data yields an age of about 5.0 ± 0.2 m.y. for the sediment/basement contact. This agrees fairly well with a recent revised estimate of 5.2 ± 0.1 m.y. for the age of the Miocene/Pliocene boundary by McDougall et al. (1977). Whether this date is directly related to the basement age at the site was not revealed by drilling, because we encountered a breccia zone beneath the sediments which extended

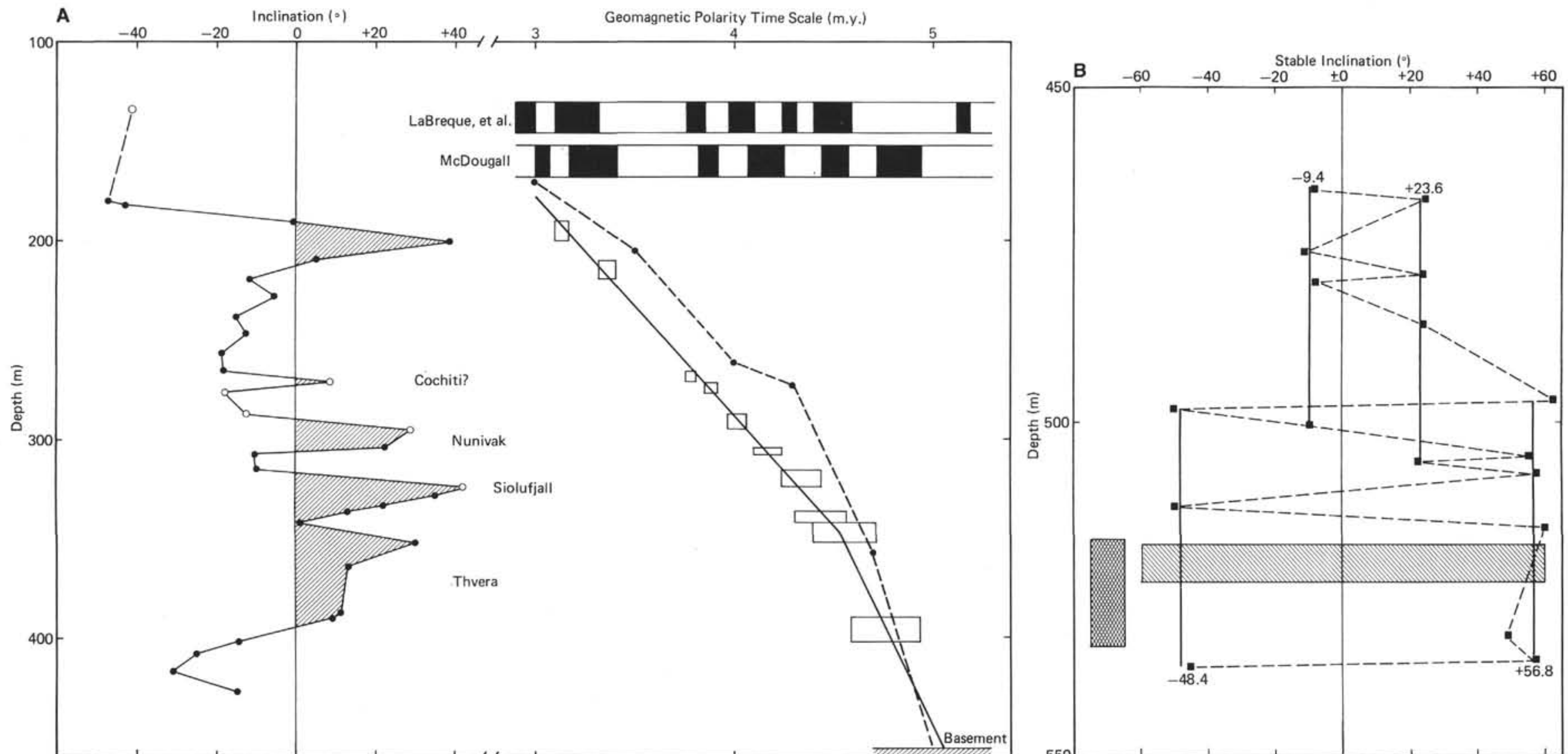

Figure 2. A. Downhole variation of magnetic inclination in Hole 453 sediments (full circles = I_{Stable}, open circles = I_{NRM}) and accumulation rate as derived from nannofossil zonation (broken line, see paleontological chapters, this volume) and magnetic polarity log of the sequence, using the paleomagnetic time scales of LaBreque et al. (1977) and McDougall (1977), both shown on top (shaded: normal polarity, white: reversed polarity). Nomenclature of polarity events according to McDougall et al. (1977). B. Downhole variation of stable magnetic inclination for Hole 453 igneous rocks. Vertical lines indicate mean values of the different inclination ranges. Shaded: "no magnetization zone" (intensity of natural remanent magnetization less than about 10^{-7} emu/cm^3). The bar on the left denotes the "hydrothermal alteration zone" as defined by petrologic criteria.

Table 2. Magnetic inclinations and paleolatitudes.[a]

	Inclinations				Latitudes			
Hole	Centered Axial Dipole	Sediments	Igneous Rocks	All Data	Present	Sediments	Igneous Rocks	All Data
453	±32.9	±21.8 ± 2.5	±36.4 ± 5.1	±23.2 ± 2.8	+17.9	±11.3 (±9.9–±12.7)	±20.2 (±16.9–±23.9)	±12.1 (±10.5–±13.7)
454A	±33.0	−23.1 ± 2.8	−25.8 ± 5.2	−24.8 ± 3.1	+18.0	±12.0 (±10.5–±13.6)	±13.6 (±10.6–±16.7)	±13.0 (±11.3–±14.8)
456	±32.9	+33.0 ± 4.6	−36.0 ± 12.3	+33.6 ± 3.6		—	—	—
456A	±32.9	±33.4 ± 3.9	—	±33.4 ± 3.9		—	—	—
Combined	±32.9	±33.2 ± 2.8	−36.0 ± 12.3	±33.5 ± 2.6	+17.9	±18.1 (±16.3–±20.0)	±20.0 (±12.4–±29.3)	±18.3 (±16.7–±20.0)
458	±32.8	±17.1 ± 2.1	±20.7 ± 4.8	±19.1 ± 2.8	+17.9	±8.7 (±7.6–±9.9)	±10.7 (±8.1–±13.4)	±9.8 (±8.3–±11.4)
Magnetic Units 1–5		—	+27.9 ± 5.0	—		—	±14.8 (±11.9–±17.9)	—
Magnetic Units 6–8		—	−8.6 ± 3.2	—		—	±4.3 (±2.7–±6.0)	—
459B	±32.8	±21.4 ± 1.0	±12.4 ± 2.2[b]	±20.6 ± 0.9	+17.9	±11.1 (±10.5–±11.6)	±6.3 (±5.1–±7.4)	±10.6 (±10.2–±11.1)
Miocene Sediments		±23.3 ± 1.2	—	—		±12.2 (±11.5–±12.8)	—	—
Oligocene Sediments		±18.0 ± 1.5	—	—		±9.2 (±8.4–±10.0)	—	—

[a] All errors listed are standard deviations of the mean.
[b] Inclination variation as representing a true reversal pattern, the respective value for a recording of paleosecular variation at an equatorial latitude becomes −0.2 ± 5.9 (see text for details).

down to the base of the hole at 605 meters sub-bottom. The close chemical affinity of these rocks to the adjacent West Mariana Ridge may indicate that they have been emplaced by a tectonic event related to an early stage of opening of the Mariana Trough. The clastic components consist predominantly of more or less extensively altered metabasalt, diabase, gabbro and, toward the base of the hole, serpentinized gabbro. The size of these clasts varies widely, gabbro pieces of several tens of centimeters long being common. With but a few exceptions, the samples for paleomagnetic measurements were taken from such megaclasts.

The remanent magnetization intensities vary from less than 10^{-7} to 7.5×10^{-3} emu/cm^3. The arithmetic mean value of 1.3×10^{-3} emu/cm^3 (s.d. 1.6×10^{-3} emu/cm^3) is only about 50 percent lower than averages previously obtained in basaltic oceanic crust (Lowrie, 1974; Ryall et al., 1977). There is no continuous downhole trend in NRM intensity, but especially low magnetization values occur in the uppermost samples and there is a zone at about 520 meters sub-bottom in which the intensities abruptly drop below the sensitivity of the magnetometer system (5×10^{-8} emu/cm^3). As with other magnetic properties (see tables in the Appendix), the most conspicuous feature of the magnetic stability is its high variability, resulting principally from the great variety of rock types and degrees of alteration represented in the breccia. Most of the samples revealed considerable amounts of spurious magnetization components; these may possibly be attributed to a secondary remanence introduced during either drilling of the main core or the minicore sampling. Their instability upon demagnetization did not substantially hinder the determination of a stable remanence direction; however, the effect largely obscures any reasonable estimate of the *in situ* magnetization state.

The general aim of the paleomagnetic study on oriented specimens from the breccia zone is to determine the emplacement temperature or to provide information about possible subsequent magnetization processes. Completely scattered magnetic directions should result from cold emplacement, without, or with, only very limited secondary magnetization components acquired after emplacement. On the other hand, hot emplacement of the breccia producing a (partial) thermoremanence (TRM), would yield coherent magnetic directions. However, some directional coherence could also be imposed on initially random magnetization directions by various secondary effects: (1) hydrothermal reheating resulting in a (partial) TRM, (2) acquisition of a viscous remanent magnetization (VRM) either at ambient or elevated temperature, and (3) alteration at ambient or elevated temperature affecting the magnetic oxide mineral assemblage and imprinting a chemical remanent magnetization (CRM). Results of stable inclinations obtained for the breccia (Fig. 2B) do not reflect a clear and simple pattern of directions but rather indicate the presence of two coherent inclination ranges. The observation is complicated by a frequent oscillation between positive and negative directions, and the fact that the negative inclinations are consistently shallower by some 10 to 15 degrees. The upper section, from the top of the breccia to about 506 meters sub-bottom, yields an average stable inclination of ±16.5° ± 7.7°. From the lower part, a mean stable inclination of ±54.0° ± 5.7° was obtained. There is a spatial overlap of both these ranges at about 500 meters sub-bottom. The overall mean stable inclination of ±36.4° ± 20.3° is in complete agreement with a centered axial dipole inclination for the present latitude of Site 453 (see Table 2). If this is a reliable result, the origin of the remanent magnetization remains obscure. Judging from the geological evidence, hot emplacement of the breccia seems highly improbable. However, some remagnetization may have occurred after emplacement. Nevertheless, any process acting at ambient temperature over a long period, would not give the observed distinct inclination ranges and mixed polarities. The close grouping around different mean directions (see Fig. 2B) may represent a spot recording of the Earth's magnetic field. Such an interpretation is consistent with the observation that none of them directly coincides with the average dipole inclination for the latitude of the site. Accepting this interpretation, a possible mechanism could have been an intense hydrothermal activity gradually declining over a long period, the different magnetic directions representing roughly two discrete blocking temperature spectra. In fact, samples carrying a shallow inclination generally display much higher magnetic stabilities compared with those of steep inclinations (see tables in the Appendix). An alternative explanation would be at least two hydrothermal episodes affecting (mainly) either the upper or the lower portion of the breccia zone. Areas of specifically low magnetic intensity where the magnetic mineral assemblage has obviously been destroyed to a great extent are likely to have acted as major pathways for the flux of hydrothermal fluids indicative of a continuous or repeated volcanic activity. The most confusing observation, which remains unexplained, is the pattern of multiple changes in magnetization polarity within a given inclination range. As matters stand, any interpretation of this most complex situation (e.g., in terms of self-reversal) would be speculative.

Site 454

This site is located in a small sediment pond, the closest suitable site (about 26 km) to the west of central graben of the Mariana Trough, the apparent axis of spreading in this back-arc basin. According to the site survey data and magnetic profiles obtained under way by the *Glomar Challenger* (see site report and underway geophysics chapter, this volume), the site is situated on a negative magnetic anomaly adjacent to the western flank of the possible central anomaly. A magnetic basement age of about 0.7 to 1.6 m.y. in the first half of the Matuyama reversed epoch, is tentatively inferred. Paleontological analysis (see Ellis, paleontological chapters, this volume) gave a sediment age of 0.9 m.y. at a subbottom depth of about 60 meters, about 8 meters above the sediment/basalt contact.

The basaltic basement includes several interlayered sediment beds. All these sediments belong to the *Gephyrocapsa caribbeanica* nannofossil Subzone (0.9–1.6 m.y.). This is in agreement with the interpretation of the magnetic anomaly pattern and would place Site 454 between the Jaramillo and Olduvai events, yielding an average basement age of 1.3 ± 0.3 m.y.

Due to a badly disturbed recovery, no paleomagnetic measurements were made on the sediments at this site, except on a few samples from mudstone beds interlayered in the basaltic basement. The upper approximately 100-meter basement section drilled consists of basaltic flows (Cores 5 and 6, and 11 and 12) interbedded with sediment layers (Cores 7 through 13), and rather poorly recovered pillowed basalts (Cores 8 through 10, and 14 through 16). Most pillow fragments recovered were too small to be positively oriented and, except for two spherulitic pillow samples from Core 16, paleomagnetic results could only be obtained from sediments and basaltic flow units.

Almost all samples studied, including the sediments, revealed magnetic stability upon AF demagnetization (MDF > 100 Oe), and only minor directional changes were observed between NRM and stable directions. Inclinations consistently became more steeply negative by several degrees upon demagnetization (see tables in the Appendix). This is thought to result from the removal of a downward-directed magnetization component that was either acquired as a VRM during the Brunhes epoch or as a spurious magnetic overprinting during drilling. On the average, almost identical remanent intensities were found for the pillows (J_{NRM} = 5.69 ± 2.47 × 10^{-3} emu/cm^3) and basaltic flows (J_{NRM} = 6.47 ± 4.61 × 10^{-3} emu/cm^3). Similar values have generally been obtained in young oceanic crust in the Atlantic (Ryall et al., 1977; Day et al., 1979), but such values are distinctly lower than those from the East Pacific Rise (Petersen, 1979). Other magnetic properties like MDF, Konigsberger ratio, and especially the initial susceptibility of the pillows and basaltic flows display systematic difference probably reflecting their different cooling history. Compared with previous DSDP results on massive oceanic flows (Bleil and Smith, 1979), the present magnetic data indicate rather thin (≲ 3-m) cooling units for the basaltic flows.

All samples, including the sediments, consistently show a negative stable inclination (Fig. 3), thus matching the sign of the magnetic anomaly at the site. This single paleomagnetic polarity of Hole 454A did not provide direct, independent age-diagnostic information. However, it is in complete agreement with the paleontologic results and the interpretation of the regional magnetic anomaly pattern as has been described in this paper.

On the basis of petrologic and geologic criteria, the basement column encountered in Hole 454A has been divided into five lithologic units. This scheme was used as a general framework to define a series of magnetic units. A magnetic unit comprises all consecutive igneous samples within a basement interval yielding a common stable inclination range. At most levels lithologic and magnetic units were found to be in excellent agreement, although lithologic Units 2 and 3 could not be verified, as no oriented samples were available from this part of the hole. On the evidence of different magnetic directions, lithologic Unit 4 was subdivided into two magnetic units (see Fig. 3 and table in the Appendix). The logging results obtained in the hole indicate, in fact, that these two magnetic units are separated by a thin sedimentary layer. Each magnetic unit is thought to repre-

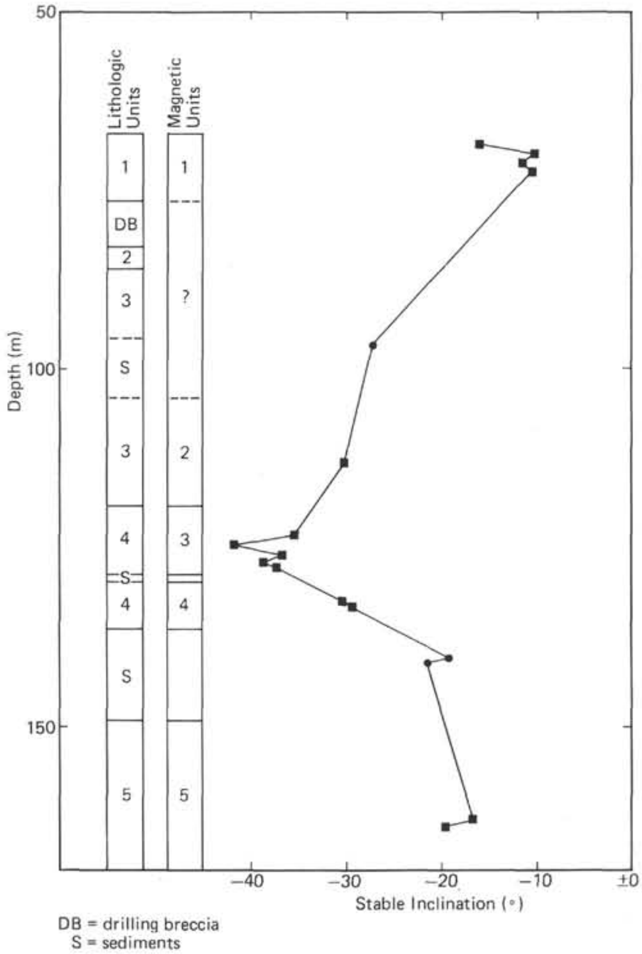

Figure 3. Downhole variation of stable magnetic inclination in the basement rocks recovered from Hole 454A (squares = basalts, circles = sediments). Columns give lithologic and magnetic units (see text for details).

sent an individual recording of the Earth's magnetic field during a separate short pulse of volcanic activity.

Estimating the thickness of the interlayered sediment beds from drilling and logging gave about 20 meters in Cores 7 through 10 and 10 meters in Cores 12 and 13, and an average sedimentation rate of 10–25 cm/10^3 y. (see paleontologic chapters, this volume). The time interval represented by the basement section drilled in Hole 454A thus amounts to about 1.2–3 × 10^5 years. Intervals between eruptions, or short eruptive sequences, at the Mid-Atlantic Ridge crest were evaluated by Ryall et al. (1977) to be of the order of 10,000 years. As at least five different magnetic/lithologic units were identified in the present hole, and there may indeed be twice this number, the present data suggest a somewhat higher average value of 1.2–6 × 10^4 years between individual pulses of volcanic activity. Together with the uniform magnetic polarity encountered, this result may put an interesting constraint on the emplacement mode of at least the extrusive portion of new crust in the Mariana Trough, as it implies a formation within a narrow zone rather than a spatially diffuse volcanism as suggested by Lawver and Hawkins (1978).

Including three sediment samples, a total of eight separate independent recordings of the Earth's paleomagnetic field directions, distributed over a span of some 100,000 years, were obtained in Hole 454A. For this reason it seems unlikely that the mean stable inclination is still biased by a large amount of secular field variation components. The average stable inclination of −24.8° (s.d. of the mean 3.1°) is significantly different from the centered axial dipole field inclination for the present latitude of the site (±33.0°), probably indicating that it has been originally situated in a more southern position. The significance of this result will be discussed in a later section.

Site 456

Two holes were drilled at Site 456 within a small sediment pond on a basement ridge about 37 km to the east of the apparent axis of spreading in the Mariana Trough (Figure 1). Hole 456A is situated some 200 meters east of the primary Hole 456. The drilling area is located on a negative magnetic anomaly, presumably between magnetic anomalies 2 (Olduvai event) and 2A (Gauss normal epoch). A basement age of 1.8 to 2.4 m.y. or 1.9 to 2.5 m.y. is therefore anticipated, using either the geomagnetic polarity time scales of LaBreque et al. (1977) or McDougall (1977), respectively. Biostratigraphic analysis in both holes gave an age of 1.6 m.y. at a sub-bottom depth of about 60 meters (see paleontologic chapters, this volume). Down to the basement contact, the entire lower sedimentary sections belong to the basement contact, the entire lower sedimentary sections belong to the nannofossil *Emiliania annula* Subzone. According to the zonation scheme of Bukry (1975), it should cover the time interval between 1.6 and 1.8 m.y. The latter date thus gives a maximum paleontological age for the sediments of Site 456.

The upper 60 meters of sediments showed significant drilling disturbance and was unsuitable for paleomagnetic study. Below this depth and including the basaltic basement, there was low recovery and most of the cores were too fragmented or disturbed by drilling to be positively oriented in the vertical sense, making them poor choices for paleomagnetic work. Conditions were somewhat better in Hole 456A sediments and Hole 456 basaltic rocks, respectively. Paleomagnetic data for the two holes are summarized in the tables in the Appendix; the downhole variation of the stable inclination direction is shown in Figure 4. The sediments in both holes were found to have a positive magnetization direction. Reversed inclinations were found in only two samples from the upper part of Hole 456A. Almost all the analyzed sediment specimens exhibited magnetic stability upon AF demagnetization, indicating that the results obtained, though scarce, are reliable.

There is no detailed correlation between the directions of magnetization in the two sedimentary sections, which is probably not surprising in view of the difficulties encountered in obtaining a representative sample collection. With exception of the uppermost two specimens in Hole 456A, all sedimentary samples ana-

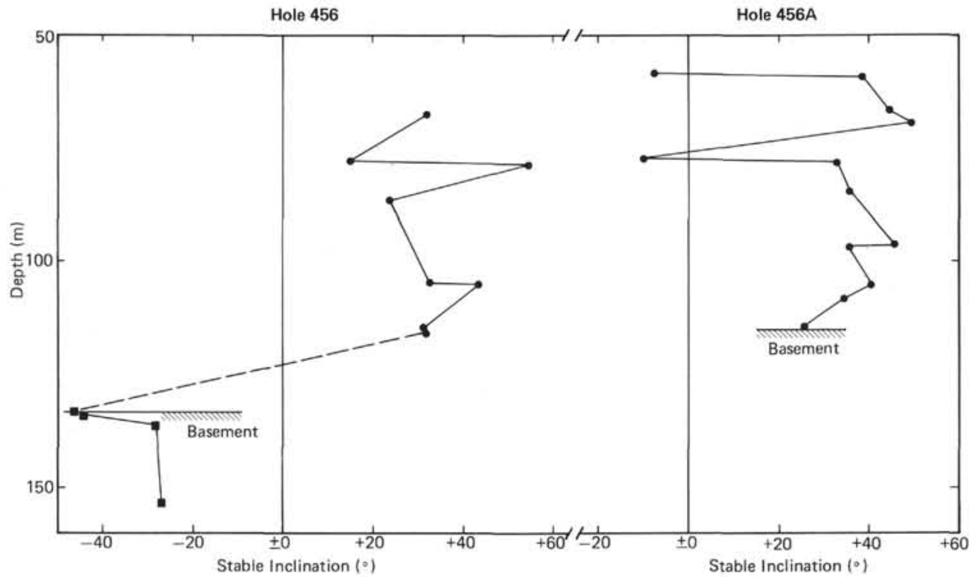

Figure 4. Downhole variation of stable magnetic inclination in Hole 456 and 456A sediments (circles) and Hole 456 basalts (squares).

lyzed have been assigned a biostratigraphic age of 1.6 to 1.8 m.y. The positive inclinations found, therefore, most likely refer to the normal Olduvai event within the reversed Matuyama epoch. The two negative inclinations encountered in Hole 456A are relatively shallow (about −10°) and may not necessarily represent a reversed Earth's magnetic field configuration. They could be explained equally well by a slightly abnormal paleosecular field behavior at this low latitude. An alternative interpretation relates Sample 5-1, 116-118 cm which belongs to the *Gephyrocapsa caribbeanica* nannofossil Subzone (0.9 to 1.6 m.y.), to the mostly reversed field (Matuyama epoch) during this period. The lower, negative Sample 7-1, 106-108 cm could be an indication that magnetic anomaly 2 consists effectively of two normal events, the Gilsa and Olduvai (see e.g., McDougall, 1977). Controversy still exists about this in the literature, and the evidence given here—based on one data point—is of course tenuous. The mean inclination of the sediments in both holes falls well within the anticipated inclination range for the present latitude of the site (see Table 2 for details).

Paleomagnetic results from the basaltic basement are available only for Hole 456. The four samples measured give a consistent reversed inclination, matching the sign of the negative anomaly at the site. In the upper few meters, the pillow basalts show features of a rather spectacular hydrothermal alteration which also affected the oxide mineralogy. There is no indication, however, that the paleomagnetic directions determined are unreliable on account of this phenomenon. A single basaltic sample from Hole 456A, tentatively oriented by vertical vesicle traces, revealed an inclination value in reasonable agreement with the other data. On the evidence of two different inclination ranges, lithologic Unit 1 was subdivided into two magnetic units, each representing a separate episode of volcanic activity. The boundary between lithologic Units 1 and 2 seems not to coincide with a magnetic boundary (see table in the Appendix), but the very limited recovery does not permit any detailed interpretation of this observation. The average stable inclination of the basalts is in good agreement with the centered axial dipole inclination for the present latitude of the site (see Table 2).

Site 458

This site is located between the presently active island arc and the mid-slope basement high in the Mariana fore-arc region (Fig. 1). The drilling area is on a slight topographic high probably related to pronounced anomalies in both gravity and magnetics (see Site Report and underway geophysics chapter, this volume). Site 458 is situated on a negative magnetic anomaly surrounded by a series of positive anomalies all reaching amplitudes of about 100 gammas, indicating a kind of dipole magnetic source layer. Similar configurations in most areas between the trench axis and the Mariana island arc, as well as the presence of seamounts, suggest that the region was built up predominantly in an arc-type setting, although no existing island arc model addresses the problem of fore-arc volcanism. Biostratigraphic analysis gave early Oligocene ages for both calcareous nannofossils and radiolarians in the lowest sediments near the basement contact in Hole 458. Accordingly, the volcanic activity here should be younger than the oldest igneous formation found on several islands of the Mariana arc. Preliminary radiometric dating of two samples (Ozima and Takigami, personal communication, 1979) gave total fusion ages of 31.8 and 40.5 m.y., respectively, but showed rather disturbed age patterns.

Similar to the situation in some of the former holes drilled during Leg 60, most of the sedimentary cores recovered at Site 458 show an extreme degree of drilling disturbance. Paleomagnetic results are thus available only from the lowest sediment section (Cores 25 through

27). Further limited by a poor magnetic stability encountered in samples near the basement contact, the paleomagnetic data obtained in the sediment column are insufficient for an interpretation in terms of magnetic dating. The average inclination is again too shallow for the present latitude of the site (see Table 2).

About 209 meters of igneous basement was successfully penetrated in Hole 458; recovery, however, was only low to moderate. The section consists of several pillow sequences and interbedded more massive flows, occasionally including fragments of limestone in the uppermost cores. Petrographically the rocks in the upper part are basaltic andesites interlayered with bronzite-andesites (Meijer et al., 1978), showing geochemical characteristics of typical island-arc volcanics (Saunders et al., 1978). Material more similar to normal oceanic tholeiites was encountered only near the base of the hole. Magnetic oxide mineralogy and several rock magnetic properties of these andesitic rocks are clearly different compared with typical ocean-floor basalts and also the basalts recovered from the Mariana Trough.

All basement samples at this site were found to be magnetically rather stable. Only minor directional variations were observed upon AF demagnetization; the median destructive field averaged 227 Oe (s.d. 77 Oe). Natural remanent magnetization intensities (J_{NRM} = 2.23×10^{-3} emu/cm^3; s.d. 4.26×10^{-3} emu/cm^3) and Königsberger ratios (Q = 4.2; s.d. 5.2) are at the lower end of ranges commonly found in oceanic rocks. The initial susceptibilities remain remarkably constant throughout (k = 1.28 emu/cm^3 • Oe; s.d. 0.41 emu/cm^3 • Oe) covering an about average distribution within the general variability in ocean-floor igneous materials. None of these magnetic properties reveals a consistent downhole trend. The samples from the last two cores (Cores 46 and 47) show a drastic increase in NRM intensity, and it is tempting to identify this interval as the top of the source layer of the magnetic anomaly. Due to various factors like low NRM intensity and Konigsberger ratio, and most important, mixed polarities, only minor contributions to the observed magnetic anomaly result from the upper basement section.

Five major lithologic units were recognized within the basement section penetrated at Site 458. In general, this division is fully confirmed by magnetic measurements (Fig. 5, table in the Appendix). As before the stable magnetic inclination was used to define the magnetic units, because it is the only magnetic property likely to remain constant over each volcanic layer erupted and cooled instantaneously on the time scale of geomagnetic variations. At two levels, a magnetic unit was found to continue about 50 cm into the lithologic unit beneath. Provided this is not due to an observational error, the most likely explanation would be a reheating of the lower unit during emplacement of the upper (younger) lava. In dividing a magmatic suite accumulated over a long period, it is crucial to know what scatter can be assigned to experimental error in the inclination data. Ryall et al. (1977) from their results on Leg 37 materials give an error of $\pm 5°$ in inclination for one sample. This total error includes effects from orientation, measurement, and determination of stable inclination. The latter procedure may effectively introduce large errors in magnetically unstable materials. For the present rocks, however, all reflecting a reasonable magnetic stability, the experimental error for a single sample probably does not exceed about 2 to 3 degrees. This estimate seems justified by the small standard deviations obtained for the inclination variation within the various magnetic units (see table in the Appendix).

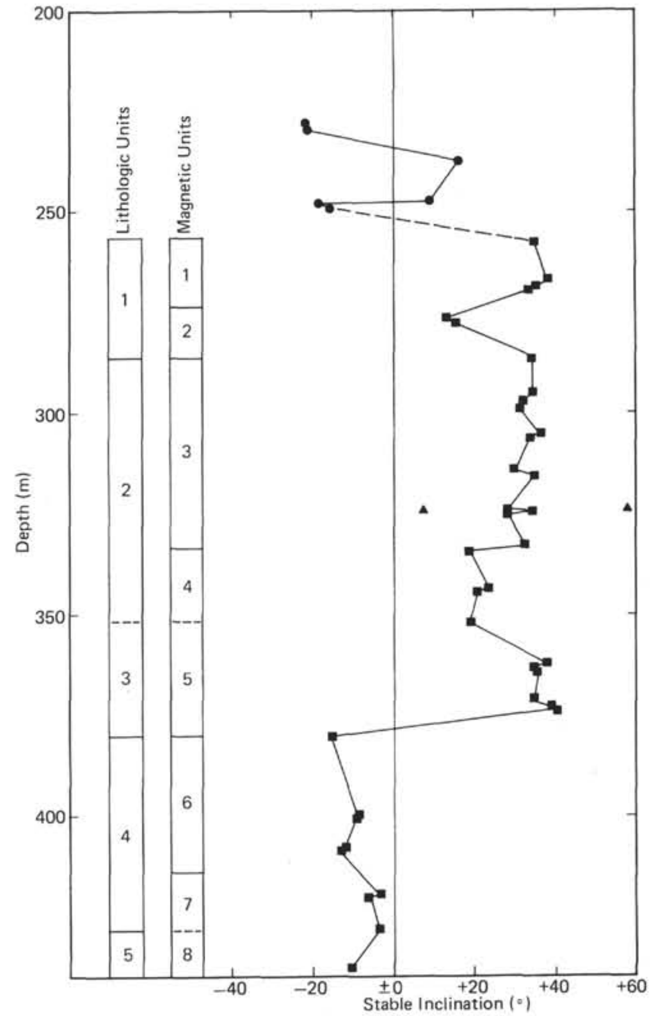

Figure 5. Downhole variation of the stable magnetic inclination for Hole 458 sediments (circles) and igneous rocks (squares); triangles denote breccia. Columns give lithologic and magnetic units. Dashed lines indicate minor discrepancies between boundaries defined by the different methods (see text for details).

On the evidence of clearly different inclination ranges, showing no overlap of the respective standard deviations, three lithologic units required subdivision into two magnetic units. On the other hand, no magnetic unit comprises more than one lithologic unit, indicating that only one magma source has been active during the same short period. This suggests a somewhat different magmatic and tectonic regime than proposed for the North Atlantic ridge. Assuming a similar magnitude of secular geomagnetic variation as observed in recent times, the present results indicate a very episodic volcanic activity as seen in most other parts of the world oceans. Individual magnetic units, some 10–50 meters thick, may represent a single eruption or an eruptional sequence over a short time span of the order of 100 years. As secular variation of the Earth's dipole and non-dipole field includes a wide range of periods, some 1000 to 100,000 years (see results of Hole 454), the intervals between different volcanic pulses should be of the same order of magnitude. This implies that where a lithologic unit required subdivision into two magnetic units, the same type of magma source prevailed over a long period without showing major evolutionary trends. On the other hand, only a small fraction of the total period in which the basement section was accumulated is represented by rock, which consequently limits the amount of magnetic information.

For the upper part, magnetic Units 1 through 5, the average stable inclination is not significantly different from a centered axial dipole inclination for the present latitude of the site. This contrasts with the shallow inclination found in the sediments, and in particular, the lower basement rocks, magnetic Units 6 through 8 (see Table 2). Due to the limited number of data, any or all the mean stable inclinations could be biased by incompletely averaged secular geomagnetic field components. Another critical factor in deciding whether a representative paleomagnetic field direction has been sampled, allowing for a reliable estimate of absolute plate motions, is to account for possible post-emplacement tectonism. The entire basement section recovered at Site 458, and especially the upper lithologic units, show extensive fracturing and numerous sheared zones; also a somewhat inclined bedding (up to 10°) was observed in the lower part of the sedimentary column.

At a sub-bottom depth of about 380 meters (between Cores 40 and 41), the stable inclinations abruptly change from positive to shallow negative without displaying intermediate, transitional directions (Fig. 5). At the same depth a lithologic break is encountered, which may mark a substantial time gap during which the earth's magnetic field reversed. Unfortunately, the contact itself was not recovered; thus, its nature remains uncertain. The abundant slickensides and highly fractured and sheared zones are indicative of a tectonic event which may account for the persistent scatter in stable inclination seen on a small scale within the magnetic units, or alternatively be evidence that a larger fault-block rotation has affected the basement section.

Site 459

This site is located just above the slope break of the Mariana Trench (Fig. 1). Magnetic site survey data revealed an extended positive magnetic anomaly in the drilling area whose nature and source are possibly related to the trench structure itself. According to the paleontological results, the oldest sediments identified were late to middle Eocene in age indicating that the basement formed at about 38–40 m.y. ago, being roughly contemporaneous with the oldest volcanics found on the Mariana island arc. One preliminary radiometric age of 36.1 ± 2.0 m.y. obtained from the igneous section at this site (Ozima and Takigami, personal communication, 1979) is based only on a rather disturbed age pattern.

With the aim of establishing a magnetic basement age and to elaborate on a possible magnetic recording of a northward movement of the region as suggested by paleomagnetics of the adjacent Site 458, at least one sample was taken from every sedimentary core section recovered in Hole 459B for paleomagnetic study. A total of 109 specimens were sampled over the 559 meters of drilled and continuously cored sediment sequence. Although a relatively high degree of drilling disturbance impaired an adequate sampling at various levels, generally the recovery allowed for a fairly well-defined vertical orientation of the specimen. Whenever possible, preference was given to areas where bedding could be used as a horizontal reference for sampling.

Among other factors, an average recovery of less than 40 per cent in the sedimentary column considerably reduced the chance of obtaining a reasonably complete polarity-age pattern in this hole. Biostratigraphic data, therefore, had to be used as calibration marks. The early Oligocene through middle Eocene is only represented by the three deepest sediment cores (Cores 58 through 60), from which almost no paleomagnetic information is available. The approximately 540 meters of sediments of Cores 1 through 57 represent the past 30 m.y. Referring to the recent polarity-time scale of LaBreque et al. (1977), the Earth's magnetic field has reversed at least 120 times during this period. Hence, on the average each core should include at least a recording of one positive and one negative geomagnetic field configuration. However, the polarity intervals are not of equal length (see Fig. 6A) and the possibility of identifying a short polarity event of the order of 0.1 m.y. is almost negligible. Extended periods ($\gtrsim$0.5 m.y.) of uniform polarity or a series of closely spaced positive or negative polarities, each of some intermediate length in general, should be represented by several data points. To some extent, therefore, the present situation is comparable to the problem of recognizing marine magnetic anomalies.

The average sedimentation rate amounts to 18 meters/m.y., but the paleontological results obtained revealed complexity in detail. From early Pliocene through middle Miocene there may have been a hiatus of 6 to 7 m.y. Another shorter hiatus of about 1 m.y. in middle/early Miocene times is probably less well-documented and not of specific relevance for the discussion of the paleomagnetic data. For most of the sediments the natural remanent magnetization intensity is of the order of 10^{-4} emu/cm^3. Upon AF demagnetization, with but a few exceptions, these samples displayed a reasonable magnetic stability, and stable magnetic directions could positively be defined using the procedures described above. Much lower NRM intensities (about 10^{-6} emu/cm^3 or less) were encountered in parts of the upper (Cores 2 through 6) and lower (Core 54 to the basement contact) sedimentary column, probably indicating a reduced volcanic ash content at these levels. Those samples frequently were found magnetically unstable, show-

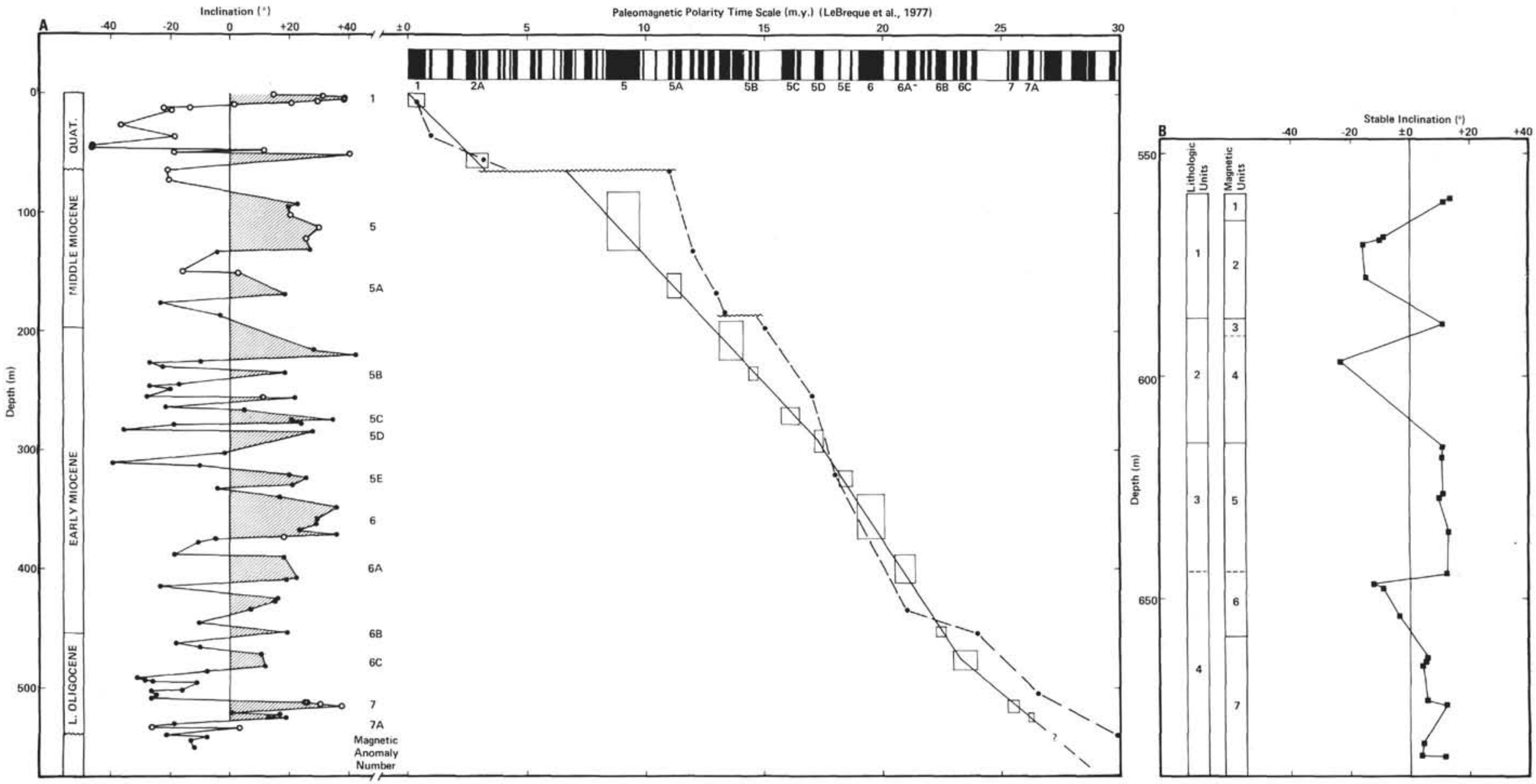

Figure 6. A. Downhole variation of the magnetic inclination in Hole 459B sediments (full circles = I_{Stable}, open circles = I_{NRM}). The column on the left gives the biostratigraphic results; the broken lines indicate the respective accumulation rate of the sediments. Straight lines show sedimentation rates as derived from the magnetic polarity log of the sequence (shaded = normal polarity, white = reversed polarity), using the paleomagnetic time scale of LaBreque et al. (1977). Only the normal polarity zones identified are indicated as columnar sections referring to the respective time and depth interval. B. Downhole variation of stable magnetic inclination in Hole 459B basement rocks. Columns give lithologic and magnetic units. Dashed lines indicate poorly confined boundaries or minor discrepancies between boundaries defined by the different methods (see text for details).

ing larger directional variations upon demagnetization, limiting a reliable definition of stable magnetic directions (see table in the Appendix).

The polarity pattern obtained (Fig. 6A) seems to be in fair agreement with established paleomagnetic time scales for most of the Cenozoic time. A magnetic downhole age scheme was based mainly on the identification of several longer periods of uniform magnetic polarity, like positive anomalies 5 and 6 and the negative interval between positive anomalies 6C and 7. Compared with the biostratigraphy, the magnetic data show almost identical trends in Quaternary, early Miocene, and late Oligocene. Differences of some 1 to 2 m.y. at some stages are probably not significant, as the presently available time scales are not yet precise enough to draw any conclusions from this evidence. A major discrepancy, however, is observed in the middle Miocene. The paleomagnetic results here give consistently younger ages and suggest that the hiatus encountered at about 65 meters sub-bottom represents only a time span of 2 to 3 m.y.

Averaging the stable inclinations of the sediments in Hole 459B again yields a mean which is too shallow for the present latitude of the site. Moreover, calculating individual averages for the Miocene and Oligocene sediments, respectively, reveals a trend toward shallower inclinations deeper in the hole—that is, with increasing age.

The igneous rocks recovered from Hole 459B are essentially clinopyroxene-plagioclase basalts. The lithologic sequence comprises pillows and interlayered, more massive flow units. The natural remanent intensities vary over almost four orders of magnitude, from 10^{-5} to 10^{-1} emu/cm^3. Thus, within only an approximately 125-meter igneous section, almost the same total range of variability is encountered as has been found in all the oceanic basement so far. The mean of $J_{NRM} = 1.4 \times 10^{-2}$ emu/cm^3 (s.d. 2×10^{-2} emu/cm^3) obtained here is the highest measured on any DSDP material. Other rock magnetic properties measured cover a more average range of values. This will be discussed in detail elsewhere.

The directional stability, though the median destructive fields are not particularly high (see table in the Appendix), was found adequate in almost all of the rocks to determine a reliable stable inclination direction.

The downhole variation of the stable inclination (Fig. 6B) in part reveals similar characteristics as seen in previous holes of this Leg. In general, there is a close correlation between lithologic and magnetic units. With one exception, all lithologic units comprise two magnetic units, suggesting that the magmatic source remained unchanged over long periods. Although the magnetic units were defined on the same basis as used before—that is, a narrow range of inclination variation over a given basement section—the downhole pattern obtained here differs from the others in that between every two magnetic units the inclination seems to change sign. This could of course be due to a somewhat peculiar mode of basement emplacement, but in view of all the other results it appears highly unlikely that the Earth's magnetic field always reversed between lithologic units and additionally several times within the unit. The downhole variation in stable inclination, therefore, may best be interpreted as reflecting in most parts a normal range of paleosecular variation of the Earth's magnetic field at an equatorial latitude. However, as indicated by the highly fractured rocks and numerous sheared zones recovered, some post-emplacement tectonism may have affected this basement section.

A mean stable inclination of $-0.2°$ (s.d. $14.4°$) is obtained, assuming the observed inclination variation is due to a normal paleosecular field variation. If the polarity pattern would entirely result from true reversals, the respective mean becomes $\pm 12.4°$ (s.d. $5.4°$). Both values clearly indicate that the site must have been at low latitude in Eocene times.

DISCUSSION AND CONCLUSIONS

The principal objectives of Leg 60 were (1) to study the mode of spreading and the character of the crust in the currently active inter-arc basin of the Mariana Trough, and (2) to trace the structural evolution of the fore-arc region of the Mariana island arc. Paleomagnetic results bearing on these different aspects were obtained from the sediment and basement rocks at three drilling sites within the Mariana Trough (Sites 453, 454, and 456) and from two holes drilled in the Mariana fore-arc area (Holes 458 and 459).

The paleomagnetic study of deep-sea sediments has led in the past to significant contributions to the magnetic reversal stratigraphy and the knowledge of paleosecular variation in the Earth's magnetic field, although only limited information is available concerning the fundamental processes by which the magnetic pattern is recorded. Various types of remanent magnetization acquisition, taking place either during deposition, postdepositional bioturbation, or chemical alteration of the sediments, may be the dominant mechanism in any particular record. Erratic remanent magnetization directions—rather frequently observed in deep-sea sediment cores—are generally believed to result from physical disturbances introduced during the coring operation. Highly unstable magnetic remanences have been found in "red clay" abyssal sediments by several workers. According to Kent and Lowrie (1974), this instability is of viscous origin and due to the presence of maghemite. No general mechanism, however, has yet been identified causing systematic deviations in magnetic directions (e.g., an inclination error). By detailed susceptibility anisotropy measurements, Kent and Lowrie (1975) showed that magnetic fabrics acquired as a result of the depositional process are almost negligible in deep-sea sediments.

Special care was taken in sampling the sediments during this Leg to avoid all disturbed zones and to refer to features of a horizontal bedding whenever possible. This safeguard, together with the overall high magnetic stability encountered, suggests that the results may represent a reliable record of the paleomagnetic field inclination. Because of the lack in azimuthal orientation of DSDP cores, reversal chronologies can only be traced by changes in sign of the inclination which may be misleading in low latitudes like the present. For the young Mariana Trough sites this probably does not introduce too much of a problem, because results of a suite of Brunhes lavas from Pagan Island (Levi et al., 1975) suggest that the Mariana region belongs to the Pacific dipole window of low angular dispersion ($<10°$) in magnetic field directions. Most of the present data apparently indicate a somewhat higher degree of variability, which in part may be due to experimental errors. Aziz-ur-Rahman and McDougall (1973) have presented evidence that the secular variation in the southwest Pacific in early Pleistocene and Pliocene times may have been higher. During this period, therefore, there may have been significant contributions from non-dipole field variations in the area. In discussing the relative magnitude in secular variation, it should be pointed out that within a sedimentary sequence covering a longer time span, possible plate motions causing a shift in magnetic mean direction must also be taken into account.

The details of the magnetic record depend upon the sedimentation rate. Low rates of about 0.1 cm/1000 y. will average out most of the secular variation in a standard sample 2.5 cm thick, whereas samples with a high accumulation rate ($\gtrsim 10$ cm/1000 y.) will record details of the paleofield variation. All sediment samples taken during this Leg apparently belong to the latter category; thus, much of the scatter seen in the data should be interpreted as the result of discontinuous spot readings of field variations. In this respect, the rather commonplace intermediate inclination values and several continuous trends in magnetic directions observed in Hole 453 and 459B sediments are difficult to understand, as they suggest much longer periods than are generally anticipated in the Earth's magnetic field secular variations.

At Site 453, adjacent to the West Mariana Ridge, which bounds the Mariana Trough to the west, the magnetic pattern in the sediments was found to match established polarity time scales in almost every detail (Fig. 2A) between approximately 3 and 5 m.y. B.P. The magnetic age of the oldest sediments (5.0 ± 0.2 m.y.) is in excellent agreement with the biostratigraphic results. Beneath the sediments, a polymict breccia layer was encountered at this site which obviously does not provide useful paleomagnetic information. The various igneous and metamorphic fragments contained in the breccia all show compositional affinity to the West Mariana Ridge igneous rocks drilled during Leg 59 (Saunders et al., 1978). This rock assemblage could have been deposited as landslide debris, or may represent the remnants of a deep-reaching fault, uplifted and exposed during the early rifting of the Mariana Trough. The drilling did not clarify whether the deeper basement at this site consists of inter-arc basin crust. Assuming it is situated on the oldest western part of the "true" Mariana Trough, the basement here should be somewhat older than the sediment age obtained. Extrapolation of spreading rates determined from the two younger Mariana Trough sites suggests an apparent basement age of about 6.5 m.y. (Fig. 7). This date places a limit on the onset of opening in this back-arc basin which, therefore, appears to be much older than previously anticipated (Karig, 1975; Karig et al., 1978).

At the two drilling sites near the center of the Mariana Trough (Sites 454 and 456), the paleomagnetic analysis did not provide independent age information. However, the magnetic pattern in the sediments and igneous rocks are again in complete agreement with paleontologic data and so it was possible to assign a magnetic basement age at both sites. The magnetic polarity in each igneous section cored was found to match the sign of the magnetic anomaly in the respective drilling area. This result, together with fairly high remanent magnetic intensities encountered, suggests that the extrusive portion of the igneous basement in the Mariana Trough effectively is a potential source layer contributing to magnetic anomaly lineations similar to those observed at mid-ocean ridges. The recent attempts by Bibee and Shor (1978) to model these anomalies may, therefore, be valid for at least the densely surveyed area near 18°N. The lack of published closely spaced geophysical profiles impairs further constraints on the detailed character of the magnetic anomaly pattern in this back-arc basin. The available data indicate a rather complex style of crustal dilation along a system of multiple short ridges and transform faults similar to the situation in the Gulf of California or the Gulf of Aden.

Figure 7 summarizes the drilling results obtained in the Mariana Trough along about 18°N. The distances of each site from the axial graben structure, the suspected locus of zero age, are plotted versus basement ages as inferred from paleomagnetic and biostratigraphic analyses. On the basis of this limited information the following tentative conclusions are drawn: (1) The apparent increase of basement ages toward the flanks of the axial zone suggests a uniaxial spreading similar to that occurring at mid-ocean ridges. (2) On the average, the spreading was symmetrical and there is no evidence for a spatially diffuse off-axis volcanism, but the accretion of new crust seems to be confined within a narrow zone at least to the central graben which has a half-width of less than 10 km at 18°N. (3) The mode of spreading was continuous with a constant (half-) rate of about 2 ± 0.5 cm/y. in Pliocene and Pleistocene times. This low spreading rate confirms the interpretation of the magnetic anomaly pattern given by Bibee and Shor (1978) and also correlates with the rough topographic relief observed. (4) The present data suggest an overall east-west spreading direction, but no further constraints of any specific strike direction on the flow lines are indicated that might decide between the different opening models proposed for the trough (Karig et al., 1978). (5) Opening of the currently active back-arc basin was initiated between about 5 and 6.5 m.y. ago. It is interesting that this date coincides approximately with a major change in direction and rate of plate motions in the Pacific region (Klitgord et al., 1975). The arcuate

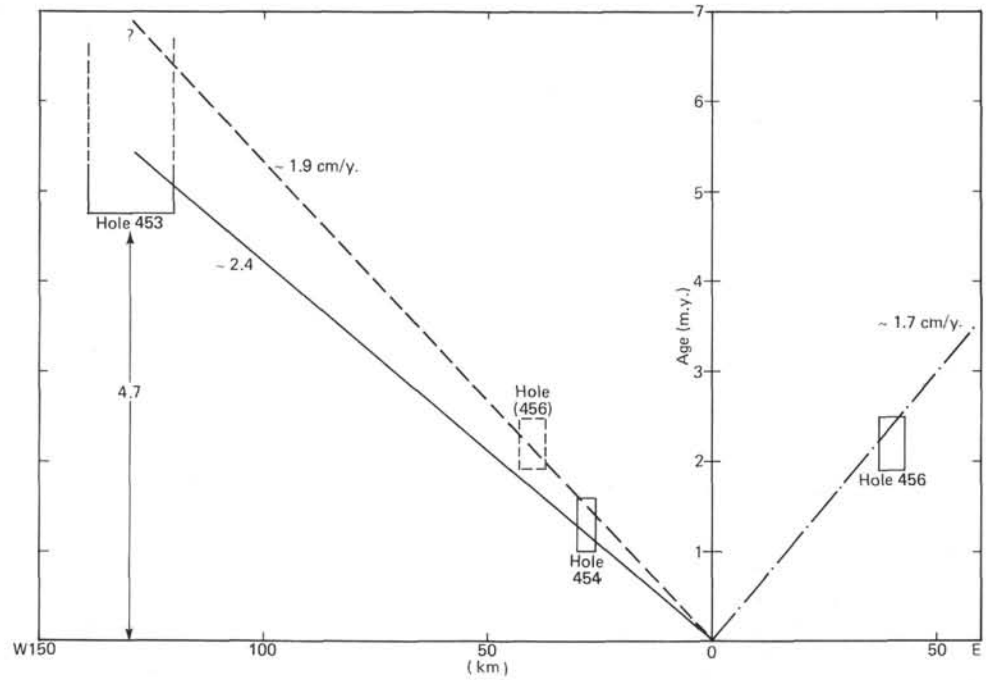

Figure 7. Distance of drilling sites (km) from the axial graben structure, the apparent spreading center in the Mariana Trough near 18°N, versus basement ages (m.y.) as inferred from paleomagnetic and biostratigraphic analyses. Error bars at each site refer to the possible age intervals and distances assuming an east-west or 30° striking flow line, respectively. Straight lines give visual best fits for constant spreading rates (see text for details). Site 456 is also shown in a hypothetical western position relative to the suggested axial zero age in the back-arc basin (broken column).

form and rotations of islands in the southern Marianas also developed since Miocene time, according to Larson et al. (1975).

As indicated in various chapters discussing results of the individual sites, with the exception of Holes 456 and 456A, all other stable remanent magnetization inclination measured for sediments and/or igneous rocks gave too shallow a mean for the present latitude of the drilling area. The simplest explanation is that their formation was at more equatorial positions (see Table 2). However, a critical assumption in the determination of paleolatitudes from the direction of remanent magnetization is that secular variation has been eliminated. Despite the high accumulation rates, only for the Hole 454A and 458 sediments, the number of samples is presumably not large enough to account for this effect. In order to avoid a bias of the averages toward shallow directions, apparent intermediate inclinations $< 10°$ for the young Mariana Trough sites and $< 5°$ for the older fore-arc sites are not included in the mean values listed in Table 2.

The situation is obviously more complicated for the different basement sections analyzed. The number of magnetic units, each representing only one independent spot recording of the Earth's paleomagnetic field, varies between two (Hole 456) and eight (Hole 458). Even in the latter case, it remains doubtful whether the mean inclination will provide a reliable reading of the axial geocentric dipole field. A further problem, in particular for the igenous rock suites, is a possible post-emplacement block rotation. A tilting resulting only in an effective 10° deflection of the median magnetic inclination would produce an error in latitude of almost the same order of magnitude for the present latitudinal position of the drilling area.

As previously described, direct evidence for some kind of tectonic event, not necessarily a tilting, was seen in the basement drill cores in Holes 458 and 459B in the Mariana fore-arc region. The Mariana Trough basement was formed at a spreading center. The results from the igneous sections here must therefore also be suspect, as a (slight) tilting is commonly associated with tectonic activity at ocean ridges. The paleolatitude obtained for Hole 454A (Table 2, Fig. 8), which is mainly based on basement rock paleomagnetics and includes only a few sedimentary data, is thus not well documented. In contrast, for Sites 453 and 456 the paleolatitudes are almost exclusively derived from sediment paleomagnetic results and should be considered reliable. According to Figure 8, for the about 2-m.y.-old Site 456, situated on the eastern spreading flank, no significant deviation from the actual latitude is indicated. Site 453 is located in the westernmost part of the Mariana Trough. Drilling could not resolve whether the basement here still belongs to the "true" Mariana Trough crust or whether it forms part of the West Mariana Ridge structure. This question, however, is crucial for any interpretation of the apparent large latitudinal offset derived from the sediment paleomagnetic results which suggest a northward motion of the drilling area by about 20 cm/y. since Miocene. Although high, this velocity is probably not totally unrealistic; its northward direction would be

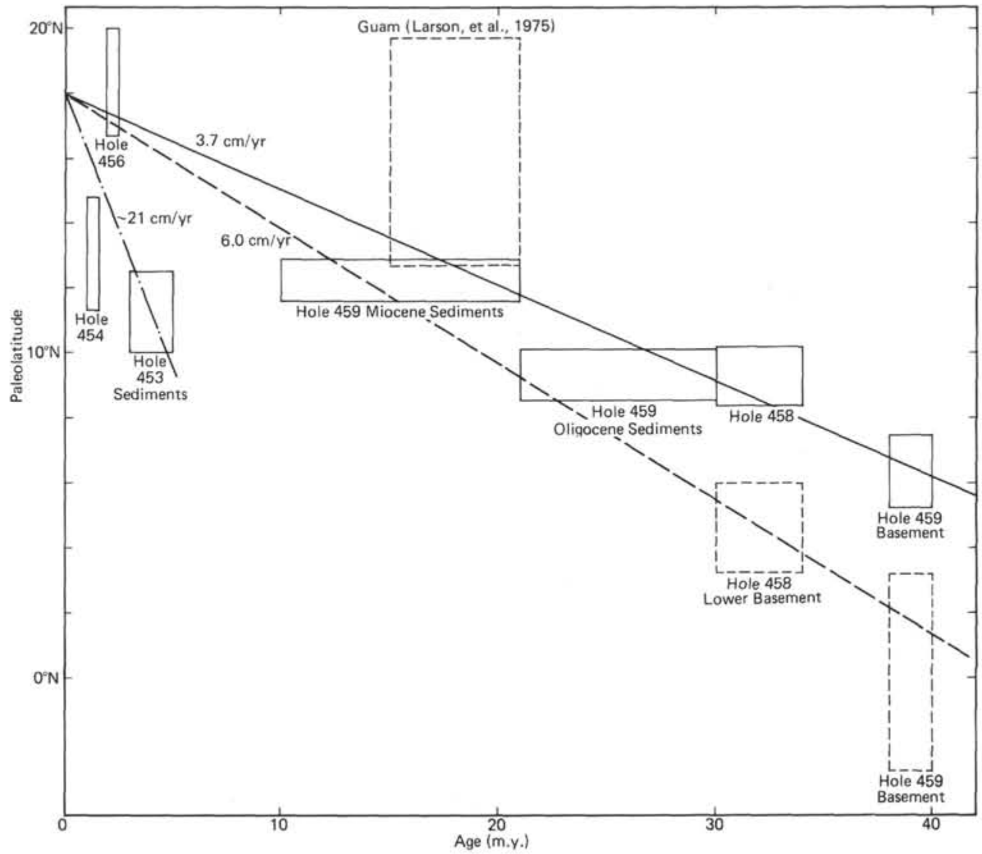

Figure 8. Age versus latitudes for Leg 60 drilling sites in the Mariana Trough (Holes 453 through 456) and Mariana fore-arc region (Holes 458 and 459). Error bars refer to age intervals as indicated by paleomagnetic and biostratigraphic results and ranges of paleolatitudes as inferred from mean inclination standard deviations (see Table 2). All present latitudes are projected to 18°N, and, unless otherwise indicated, paleolatitudes given were deduced from combined paleomagnetic data of sediments and igneous rocks. In addition, results from Guam Island (Larson et al., 1975) are plotted. Straight lines indicate different visual best fit estimates for a continuous northward movement of the drilling area (see text for details).

compatible with a large post-Miocene clockwise tectonic rotation (about 50°) of the entire southern Mariana arc-trench system as indicated by paleomagnetic data from Guam (Larson et al., 1975) and possibly Saipan (Dunn et al., 1979). Results of the West Philippine Basin (Louden, 1977) from both a paleomagnetic study of DSDP sediment cores and phase shifting of marine magnetic anomalies gave strong evidence for a considerable northward movement of the Philippine plate during the past 50 m.y., including a large rotational component (about 60°). If the same general plate motion is effectively documented in the Mariana area as proposed by Louden (1977), this would imply that it has not been completely disrupted by inter-arc spreading episodes between the Mariana Arc and the West Philippine Basin. On the other hand this idea, like the present results from Hole 453, seems to be in conflict with any opening model proposed so far for the Mariana Trough (Karig et al., 1978).

Paleomagnetic results from both drilling sites in the Mariana fore-arc also clearly indicate some northward movement of this area. The data are summarized in Table 2 and Figure 8. In particular, the magnetic records obtained from the Hole 459B sediments provide detailed information about the latitudinal variation in Oligocene and Miocene times. In the sedimentary column of this hole the paleomagnetic and biostratigraphic age pattern identified shows generally a nearly perfect correlation (Fig. 6A). Because of the close interrelationship of the respective time scales, the apparent large discrepancy around magnetic anomaly 5—where the paleontologic results indicate considerable older ages—is rather surprising. However, similar observations have also been reported from other DSDP sites (LaBreque et al., 1977). As the time of magnetic anomaly 5 is controlled by radiometric dating, it appears that the biostratigraphic zonation scheme needs revision for this period.

The mean inclination of the sediments shows a gradual shallowing with increasing age in Hole 459B. This trend is confirmed by the basement paleomagnetics at both fore-arc drilling sites. The respective variation in latitudes is illustrated in Figure 8. To allow for a direct comparison of the different results, all present latitudes have been projected to 18°N. As the various data points all cover a more or less extended time interval, and some error has to be assigned to the latitudes according to the standard deviations in mean inclinations, the northward movement—though well documented as a general feature—cannot be traced exactly in space and time. Different best visual fits, assuming a constant continuous motion from Eocene to present, are shown in Figure 8. The resulting velocities are in fair agreement with those obtained from the West Philippine Basin (Louden, 1977), but as already indicated by his data and the paleomagnetic results from the Mariana island arc (Larson et al., 1975; Levi et al., 1975; Dunn et al., 1979), most of the northward movement could have been completed before Miocene times.

In conclusion, the different results may also place some interesting constraints on the opening mode of the Mariana Trough. The eastern portion, including the island arc and fore-arc region, has apparently undergone only a limited northward motion at least in the past 5 m.y. Results from the western half of the trough (Sites 453 and 454), on the other hand, strongly suggest a marked latitudinal motion to the north. A possible interpretation, therefore, would be that spreading even in this central portion of the Mariana Trough at 18°N was approximately in a northwest-southeast direction, a relative northward motion being superimposed, probably associated with a clockwise rotational component.

ACKNOWLEDGMENTS

I would like to thank the many people who were responsible for the success of DSDP Leg 60. Prof. J. Untiedt kindly made available the paleomagnetic laboratory facilities at the University of Munster, Germany. I am also grateful to N. Weinreich and H. U. Worm for assistance with the measurements and to R. Day and M. Fuller for review of the manuscript.

This study was made possible by funds provided by the Deutsche Forschungsgemeinschaft.

REFERENCES

Ade-Hall, J. M., and Johnson, H. P., 1976. Paleomagnetism of basalts, Leg 34. *In* Yeats, R. S., Hart, S. R., et al., *Init. Repts. DSDP*, 34: Washington (U.S. Govt. Printing Office), 513-532.

Aziz-Ur-Rahman, and McDougall, I., 1973. Paleomagnetism and paleosecular variation on lavas from Norfolk and Philip Islands, southwest Pacific Ocean. *Geophys. J.*, 33:141-156.

Bibee, L. D., and Shor, G. G., 1978. *IPOD Site Survey Along the South Philippine Sea Transect:* unpublished report.

Bleil, U., and Smith, B. M., 1979. Paleomagnetism of basalts Leg 51. *In* Donnelly, T. W., Francheteau, J., Bryan, W., Robinson, P., Flower, M., Salisbury, M., et al., *Init. Repts. DSDP*, 51, 52, 53, Pt. 2: Washington (U.S. Govt. Printing Office), 1351-1361.

Bukry, D., 1975. Coccolith and silicoflagellate stratigraphy, northwestern Pacific Ocean, Deep Sea Drilling Project, Leg 32. *In* Larson, R. L., Moberly, R., et al., *Init. Repts. DSDP*, 32: Washington (U.S. Govt. Printing Office), 677-701.

Day, R., Halgedahl, S., Steiner, M., Kobayashi, K., Furuta, T., Ischii, T., and Faller, A., 1979. Magnetic properties of basalts from DSDP Leg 49. *In* Luyendyk, B. P., Cann, J. R., et al., *Init. Repts. DSDP*, 49: Washington (U.S. Govt. Printing Office), 781-791.

Dunn, J. R., Fuller, M., Green, G., McCabe, R., and Williams, I., 1979. Preliminary paleomagnetic results from the Philippines, Marianas, Carolines and Solomons. *Am. Geophys. Union Trans.*, 60:239. (Abstract)

Karig, D. E., 1971. Structural history of the Mariana Island arc system. *Geol. Soc. Am. Bull.*, 82:323-344.

________, 1975. Basin genesis in the Philippine Sea. *In* Karig, D. E., Ingle, J. C., Jr., et al., *Init. Repts. DSDP*, 31: Washington (U.S. Govt. Printing Office), 857-879.

Karig, D. E., Anderson, R. N., and Bibee, L. D., 1978. Characteristics of back arc spreading in the Mariana Trough. *J. Geophys. Res.*, 83:1213-1226.

Karig, D. E., and Glassley, W. E., 1970. Dacite and related sediment from the West Mariana Ridge, Philippine Sea. *Geol. Soc. Am. Bull.*, 81:2143-2146.

Kent, D. V., and Lowrie, W., 1974. Origin of magnetic instability in sediment cores from the Central North Pacific. *J. Geophy. Res.*, 79:2987-3000.

________, 1975. On the magnetic susceptibility anisotropy of deep-sea sediment. *Earth Planet. Sci. Lett.*, 28:1-12.

Klitgord, K. D., Huestis, S. P., Mudie, J. D., and Parker, R. L., 1975. An analysis of near-bottom magnetic anomalies: Sea floor spreading and the magnetized layer. *Geophys. J.*, 43:387-424.

LaBreque, J. L., Kent, D. V., and Cande, S. C., 1977. Revised magnetic polarity time scale for Late Cretaceous and Cenozoic time. *Geology*, 5:330-335.

Larson, E. E., Reynolds, R. L., Ozima, M., et al., 1975. Japan-U.S. paleomagnetism project in Micronesia. Paleomagnetism of Miocene volcanic rocks of Guam and the curvature of the Southern Mariana Island arc. *Geol. Soc. Am. Bull.*, 86:346-350.

Lawver, L. A., and Hawkins, J. W., 1978. Diffuse magnetic anomalies in marginal basins: Their possible tectonic and petrologic significance. *Tectonophysics*, 45:323-339.

Levi, S., Merrill, R., Aoki, Y., et al., 1975. U.S.-Japan cooperation program in Micronesia. Paleosecular variation of lavas from the Marianas in the western Pacific Ocean. *J. Geomag. Geoeletr.*, 27:57-66.

Louden, K. E., 1977. Paleomagnetism of DSDP sediments, phase shifting of magnetic anomalies, and rotations of the West Philippine Basin. *J. Geophys. Res.*, 82:2989-3002.

Lowrie, W., 1974. Oceanic basalt magnetic properties and the Vine and Matthews hypothesis. *J. Geophys.*, 40:513-536.

McDougall, I., 1977. *The Present Status of the Geomagnetic Polarity Time Scale:* Canberra (Austr. Nat. Univ., Res. School Earth Sci.), Publ. No. 1288.

McDougall, I., Saemundson, K., Johannesson, H., Watkins, N. D., and Kristjansson, L., 1977. Extension of the geomagnetic polarity time scale to 6.5 m.y.: K-Ar dating, geological and paleomagnetic study of a 3,500 m lava succession in western Iceland. *Geol. Soc. Am. Bull.*, 88:1-15.

Meijer, A., and Shipboard Scientific Party IPOD, Leg 60, 1978. Petrology of volcanic rocks from the Mariana arc-trench gap and gabbros from the Mariana inter-arc basin, IPOD, Leg 60. *Am. Geophys. Union Trans.*, 59:1182. (Abstract)

Petersen, N., in press. Paleomagnetism and rock magnetism of basalts, Leg 54. *In* Hekinian, R., Rosendahl, B. R., et al., *Init. Repts. DSDP*, 54: Washington (U.S. Govt. Printing Office).

Ryall, P. J. C., Hall, J. M., Clark, J., and Milligan, T., 1977. Magnetization of oceanic crustal layer 2—results and thoughts after DSDP Leg 37. *Can. J. Earth Sci.*, 14:684-706.

Saunders, A. D., Marsh, N. G., and Tarney, J., 1978. Geochemistry of arc and inter-arc basalts from the east Mariana transect: IPOD Leg 60. *Am. Geophys. Union Trans.*, 59:1182. (Abstract)

Zijderveld, J. D. A., 1968. A. C. demagnetization of rocks: Analysis of results. *In* Collison, D. W., Creer, K. M., and Runcorn, S. K., (Eds.), *Methods in Paleomagnetism:* Amsterdam (Elsevier Scientific Publ. Co.), pp. 254-286.

APPENDIX

This section lists paleomagnetic parameters on a sample-by-sample basis for the sediments (Table 1) and basement rocks (Table 2). For the igneous samples also basic rock magnetic properties are listed.

Table 3 summarizes the lithologic and magnetic stratigraphy for the drill holes. Upper and lower limits of magnetic units refer to first and last sample measured; errors listed for stable inclinations are standard deviations.

Table 1. Results of paleomagnetic measurements of Leg 60 sediments.

Sample (interval in cm)	Depth below Sea Floor (m)	J_{NRM} (10^{-6} emu/cm^3)	I_{NRM}	I_{Stable}	D_{NRM}	D_{Stable}
Hole 453						
15-2, 16–18	134.17	~0.1	−41.1	no	14.3	no
19,CC, 5–8	179.87	136	−40.7	−47.1	223.8	228.7
20-2, 58–60	182.09	~0.1	−14.9	(−42.7)	259.9	(239.7)
21-1, 100–103	190.52	61.1	+0.3	−0.7	84.2	84.0
22-2, 17–20	200.69	195	+35.8	+38.9	148.6	145.9
23-1, 89–91	209.40	6.3	+6.0	+5.3	178.2	175.7
24-1, 137–140	219.39	3.3	+1.8	−11.6	142.0	142.1
25-1, 118–120	228.69	49.2	−0.9	−5.1	252.8	260.6
26-2, 7–9	238.58	40.4	−12.1	−14.8	342.8	340.0
27-1, 23–25	246.74	85.8	−7.6	−12.2	125.9	119.8
28-1, 29–31	256.30	7.0	−21.1	−18.6	180.1	180.0
29-1, 24–26	265.75	244	−13.2	−18.2	23.3	27.4
29-4, 69–71	270.70	<0.1	+8.7	—	86.0	—
30-1, 92–94	275.93	<0.1	−17.8	—	184.6	—
31-2, 81–83	286.92	<0.1	−12.5	—	82.1	—
32-1, 74–76	294.75	<0.1	+28.8	—	90.0	—
33-1, 59–61	304.10	57.1	+14.7	+22.5	7.3	7.0
33-3, 81–83	307.32	~0.1	+79.6	(−10.5)	231.7	(101.4)
34-2, 21–23	314.72	2.5	+3.4	(−9.9)	257.4	(262.9)
35-1, 126–128	323.77	<0.1	+42.0	—	333.6	—
35-4, 101–103	328.02	695	+32.1	+35.2	64.4	64.0
36-1, 82–84	332.83	26.8	+17.0	+21.6	106.4	96.1
36-3, 131–133	336.32	0.4	+11.7	+12.8	345.4	351.0
37-1, 18–20	341.69	179	+1.2	+0.6	262.6	261.7
38-1, 46–48	351.47	78.1	+28.9	+31.0	269.6	269.8
39-3, 59–61	364.10	4.0	+10.6	+13.3	101.9	101.3
41-5, 120–122	386.71	216	+22.2	+11.4	293.0	283.3
42-1, 54–56	389.55	196	+18.8	+9.2	174.9	176.7
43-3, 19–21	401.70	0.3	−1.7	−14.5	112.2	100.8
44-1, 65–67	408.66	1.2	−16.1	−24.7	14.7	10.6
45-1, 7–9	417.58	29.5	−27.5	−30.9	187.5	189.3
46-1, 19–21	427.20	186	−10.2	−14.5	95.1	92.8
47-3, 8–10	439.59	<0.1	—	—	—	—
48-1, 12–14	446.13	<0.1	—	—	—	—
Hole 456						
9-1, 59–61	67.60	122	+36.4	+31.4	122.9	108.5
10-1, 117–119	77.68	109	+14.9	+14.7	161.5	168.8
10-2, 64–66	78.65	89.1	+65.2	+55.1	341.8	299.4
11-1, 54–56	86.55	81.4	+28.6	+23.4	299.5	299.9
12,CC, 3–4	104.84	111	+37.9	+32.4	157.2	153.0
13-1, 25–27	105.26	2.52×10^{-3}	−34.2	+43.5	131.1	131.6
14-1, 7–9	114.58	121	+39.7	+31.5	148.7	150.2
14-1, 73–75	115.24	120	+36.8	+31.9	296.0	296.4
Hole 456A						
5-1, 116–118	58.17	145	+9.1	−7.8	289.1	285.7
5-2, 108–110	59.59	174	+35.5	+38.2	50.5	55.8
6-1, 64–66	67.15	118	+38.3	+44.6	256.2	250.4
6-2, 106–108	69.07	117	+40.7	+49.3	56.0	56.2
7-1, 104–106	77.05	111	−2.7	−10.5	151.4	152.0
7-2, 58–60	78.09	132	+34.8	+33.0	144.1	145.9
8-1, 39–41	85.90	695	+33.5	+35.7	89.3	89.8
9-1, 139–141	96.40	132	+42.3	+45.9	56.2	63.2
9-2, 35–37	96.86	111	+23.6	+35.3	338.2	353.9
10-1, 41–43	104.92	159	+34.4	+40.4	229.7	232.8
10-3, 59–61	108.10	156	+36.6	+34.2	140.5	142.4
11-1, 57–59	114.58	64.6	+27.9	+25.3	52.3	49.7
Hole 458						
25-1, 46–48	228.47	57.5	−15.8	−21.8	72.2	67.7
25-2, 48–50	229.99	86.2	−21.0	−21.7	7.8	3.6
26-1, 28–30	237.79	110	+28.2	+15.8	128.5	133.0
27-1, 35–37	247.36	16.3	+19.8	(+9.2)	40.1	(15.6)
27-1, 106–108	248.07	1.4	+51.6	(−18.3)	326.5	(185.7)
27-2, 29–31	248.80	8.2	−55.8	(−15.6)	162.7	(59.5)
Hole 459B						
1-1, 130–132	1.31	91.5	+14.4	—	120.0	—
1-2, 99–101	2.50	74.0	+31.2	—	21.3	—
1-3, 78–80	3.79	71.5	+38.5	—	13.5	—
1-4, 34–35	4.85	83.3	+38.1	—	81.4	—
1-5, 8–10	6.09	68.0	+29.2	—	101.7	—
2-1, 43–45	7.94	0.3	+20.8	—	237.3	—
2-2, 30–32	9.31	~0.1	+1.6	—	268.4	—
2-3, 104–106	11.55	0.3	−13.5	—	180.1	—
2-4, 34–36	12.35	~0.1	−22.0	—	220.7	—
2-5, 10–12	13.61	0.2	−19.5	—	354.5	—
4,CC, 11–13	26.62	168	−36.5	—	352.8	—
5-1, 9–10	36.09	1.5	−19.0	—	209.5	—
6-1, 128–130	46.79	5.8	−46.1	—	352.3	—
6-2, 84–86	47.85	~0.1	−46.4	—	355.1	—
6-3, 67–69	49.18	117	+11.2	—	30.0	—
6-4, 11–13	50.12	0.2	−19.0	—	0.1	—
6,CC, 12–14	51.28	<0.1	+39.6	—	198.1	—
8-1, 140–142	65.91	367	−21.0	—	358.2	—
9-1, 58–60	74.59	778	−20.7	—	291.4	—
11-1, 47–49	93.48	347	+18.6	+22.9	226.1	226.0
11-2, 53–55	95.04	443	+18.8	+19.2	97.1	96.3
12,CC, 19–21	102.70	162	+19.8	—	305.2	—
13-1, 77–79	112.78	171	+30.1	—	3.6	—
14-1, 55–57	122.06	378	+25.4	—	350.1	—

Table 1. (Continued).

Sample (interval in cm)	Depth below Sea Floor (m)	J_{NRM} (10^{-6} emu/cm^3)	I_{NRM}	I_{Stable}	D_{NRM}	D_{Stable}
Hole 459B						
15-1, 22–24	131.23	83.3	+47.3	(+27.0)	228.8	(181.5)
15-2, 136–138	133.87	117	−4.4	−4.6	35.5	13.3
17-1, 13–15	150.14	138	−15.9	—	20.7	—
17,CC, 7–9	151.33	224	+2.8	—	16.0	—
19-1, 12–14	169.13	125	+22.2	+18.2	287.8	277.5
20-1, 40–42	178.91	99.0	−17.3	−23.6	129.9	101.6
21-1, 80–82	188.81	255	−15.4	−12.8	215.2	216.3
24-1, 9–11	216.60	115	+29.6	+28.2	134.1	152.7
24-2, 14–16	218.15	120	+42.1	+42.0	306.1	310.0
25-1, 49–51	226.50	191	−6.0	−10.1	270.0	89.2
25-2, 40–42	227.91	117	−41.6	−27.5	113.7	281.9
25-3, 92–94	229.93	93.8	−40.7	−22.6	119.5	90.2
26-1, 33–35	235.84	110	+15.6	+18.3	151.1	179.8
27-1, 8–10	245.09	129	−24.2	−17.0	149.8	161.1
27-2, 33–35	246.84	39.7	−10.6	(−27.4)	247.4	(193.2)
27-3, 99–101	249.00	74.4	−21.8	−19.6	21.5	348.5
27-4, 143–145	250.94	107	−15.9	−19.8	244.3	254.4
28-1, 13–15	254.64	109	−24.8	−28.2	29.2	6.6
28-2, 62–64	256.63	28.9	+11.5	—	266.8	—
28-3, 102–104	258.53	157	+21.7	+21.9	247.2	254.4
29-1, 22–24	264.23	123	−21.0	−22.1	224.6	208.2
29-2, 86–88	266.37	72.1	−41.9	(+4.6)	94.6	(92.8)
30-1, 64–67	274.16	117	+48.3	(+34.4)	26.8	(0.4)
30-2, 46–49	275.48	219	+19.7	+20.8	5.1	4.3
30-3, 100–103	277.52	249	+21.7	+24.8	125.4	126.2
30-4, 91–94	278.93	106	+27.9	−18.7	33.8	25.3
31-1, 114–115	284.15	108	−31.5	−35.7	348.7	3.9
31-2, 78–80	285.29	134	+34.7	+28.1	292.3	293.2
33-1, 12–15	302.14	272	−1.3	−1.6	265.5	268.9
34-1, 10–12	311.61	627	−50.9	−39.9	16.0	20.4
34-2, 28–30	313.29	266	+1.8	−10.2	70.6	80.0
35-1, 23–25	321.24	117	+17.5	+20.6	55.4	72.3
35-2, 139–141	323.90	113	+30.9	+26.3	69.6	83.3
36-1, 18–20	330.69	112	+25.7	+21.0	265.6	268.3
36-2, 70–72	332.71	80.3	+9.1	−4.4	77.0	79.5
37-1, 19–20	340.20	84.5	+14.8	+16.9	192.6	182.5
38-1, 34–36	349.85	136	+43.7	+35.6	338.7	353.4
39-1, 12–14	359.13	110	+26.2	+29.3	250.2	254.5
39-2, 61–63	361.12	119	+42.6	+29.0	72.4	88.9
40-1, 4–6	368.55	85.2	+26.3	+23.5	154.9	175.2
40-2, 128–130	371.29	103	+31.2	+35.8	220.7	226.8
40-3, 15–17	371.66	32.1	+18.1	—	230.4	—
40-4, 106–108	374.07	96.3	−0.6	−5.0	330.0	349.0
41,CC, 18–20	378.19	58.4	−6.7	−10.8	73.0	86.7
42-1, 40–42	387.91	39.2	−7.1	(−18.4)	4.9	(6.9)
42-2, 73–75	389.74	163	+6.4	+18.9	234.4	239.0
42-3, 23–25	390.74	109	+26.0	+18.6	74.5	85.0
44-1, 69–71	407.20	41.4	+22.8	+22.4	208.2	197.0
44-2, 52–54	408.53	103	+32.7	+19.3	248.9	269.3
45-1, 6–8	416.07	177	−25.1	−24.2	213.7	208.3
46-1, 20–22	425.71	122	+15.6	+16.3	326.3	344.1
46-2, 102–104	428.03	165	+13.3	+15.4	288.9	279.5
47-1, 59–61	435.60	104	+7.3	+6.1	137.9	141.5
48-1, 85–87	445.36	806	−14.1	−16.1	209.9	209.4
49-1, 27–29	454.28	82.9	+42.1	+19.0	55.8	16.2
50-1, 25–27	463.76	92.7	−27.2	−19.1	340.5	350.1
50-2, 104–106	466.05	222	−16.2	−9.9	94.5	90.8
51-1, 15–17	473.16	27.6	−6.7	(+11.0)	19.1	(18.9)
52-1, 6–8	482.57	41.9	+22.0	+11.5	314.5	319.2
52,CC, 25–57	486.50	51.7	−10.1	−8.0	24.5	9.9
53-1, 79–81	492.80	22.5	−34.2	−31.4	234.5	90.0
53-2, 25–27	493.76	86.8	−33.9	−28.8	243.3	255.3
53-3, 62–64	495.63	112	−36.9	−26.5	87.7	88.5
53-4, 46–48	496.97	34.2	−17.1	−11.0	266.8	268.2
54-1, 58–60	502.09	6.5	−10.4	(−16.5)	16.8	(180.0)
54-2, 45–47	503.46	7.7	−49.3	−27.1	330.4	327.6
54-3, 42–44	504.93	4.4	−3.5	(−26.2)	92.5	(191.2)
54-4, 65–67	506.66	20.6	−24.0	−25.0	171.8	172.2
54-5, 52–54	508.03	92.4	−31.4	−26.8	156.3	166.9
55-1, 78–80	511.79	<0.1	+25.1	—	237.0	—
55-2, 17–19	512.68	<0.1	+25.6	—	7.6	—
55-3, 28–30	514.29	~0.1	+30.0	—	311.0	—
55-4, 64–66	516.15	<0.1	+36.8	—	341.9	—
56-1, 55–57	521.06	<0.1	+14.1	(−0.2)	246.5	(90.1)
56-2, 80–82	522.81	<0.1	+42.4	+17.2	136.7	174.8
56-3, 68–70	524.19	3.4	+5.7	+12.8	200.3	219.2
56-4, 69–71	525.70	27.0	+23.1	+18.3	282.8	273.1
57-1, 34–36	530.36	0.7	−8.5	(−19.1)	101.9	(143.6)
57-2, 68–70	532.19	2.3	−36.9	−25.8	19.6	1.3
57-3, 64–66	533.65	<0.1	−27.1	—	298.4	—
57,CC, 15–17	533.76	0.3	+2.8	—	103.7	—
58-1, 68–70	540.19	46.8	−15.6	−21.7	182.6	180.7
58-2, 58–60	541.59	72.8	−2.9	−7.4	182.0	180.6
58-3, 75–77	543.26	0.4	−54.9	(−13.5)	163.8	(96.3)
59-2, 33–35	550.84	86.5	−6.1	−11.9	93.6	92.6

Notes:

I_{NRM}, D_{NRM} = directions of natural remanent magnetization; I = inclination in degrees with respect to horizontal, negative above horizon; D = declination in degrees with reference to an arbitrary zero azimuth.

I_{Stable}, D_{Stable} = stable magnetization directions as resulting from an AF or thermal demagnetization analysis, brackets indicate a limited degree of reliability.

Table 2. Results of paleomagnetic measurements of Leg 60 basement rocks.

Sample (interval in cm)	Depth below Sea Floor (m)	J_{NRM} (emu/cm^3)	I_{NRM}	I_{Stable}	D_{NRM}	D_{Stable}	MDF (Oe)	k	Q
Hole 453									
49-1, 110–113	456.62	7×10^{-6}	+58.7	no	167.6	no	48	59×10^{-6}	0.3
50-1, 39–42	465.41	23×10^{-6}	−7.2	−8.4	225.2	236.8	125	69×10^{-6}	0.9
50-2, 40–43	466.92	2.18×10^{-3}	+17.1	+24.4	309.0	315.9	361[b]	0.449×10^{-3}	13.1
51-1, 8–11	474.60	1.85×10^{-3}	+2.2	−11.3	240.2	241.7	538	1.95×10^{-3}	2.6
51-3, 50–52	478.01	2.41×10^{-3}	+10.7	+23.9	243.9	262.2	281	1.85×10^{-3}	3.5
51-4, 7–10	479.09	7.50×10^{-3}	−2.2	−8.2	80.7	78.4	548	1.68×10^{-3}	12.1
52-2, 13–16	485.65	0.442×10^{-3}	+22.4	+23.9	110.8	108.3	270	0.268×10^{-3}	4.5
53-3, 28–31	496.80	1.44×10^{-3}	+56.1	(+62.6)	183.5	(197.3)	58	3.68×10^{-3}	1.1
53-4, 5–8	498.07	0.442×10^{-3}	+55.1	−49.6	150.3	87.5	64	1.50×10^{-3}	0.8
53-5, 121–123	500.72	34×10^{-6}	+4.3	(−9.8)	110.7	(102.8)	55	0.544×10^{-3}	0.2
54-2, 67–69	505.18	1.28×10^{-3}	+47.0	+55.0	167.8	155.8	278	6.27×10^{-3}	0.6
54-3, 5–8	506.07	0.765×10^{-3}	+65.8	(+22.2)	155.4	(14.0)	61	3.46×10^{-3}	0.6
54-4, 16–19	507.68	1.28×10^{-3}	+64.3	(+57.3)	166.2	(161.7)	256	2.51×10^{-3}	1.4
55-1, 6–8	512.57	2.85×10^{-3}	−46.1	(−50.1)	176.3	(161.0)	56	4.81×10^{-3}	1.6
55-3, 28–31	515.80	2.35×10^{-3}	+59.7	+59.7	175.7	190.8	339	5.18×10^{-3}	1.2
55-4, 141–143	518.42	$<10^{-7}$	—	—	—	—	—	—	—
56-1, 42–44	522.43	$<10^{-7}$	—	—	—	—	—	—	—
56-2, 36–39	523.88	$<10^{-7}$	—	—	—	—	—	—	—
57-1, 88–91	532.40	1.03×10^{-3}	+43.9	+49.0	156.9	113.0	77	3.35×10^{-3}	0.8
57-3, 111–113	535.62	1.29×10^{-3}	+57.3	+57.2	235.2	262.1	507	1.55×10^{-3}	2.3
57-4, 59–62	536.61	0.919×10^{-3}	+7.1	−45.6	193.9	207.1	133	2.01×10^{-3}	1.2
63-1, 11–13	588.62	0.878×10^{-3}	+39.5	—	208.8		49	4.99×10^{-3}	0.5
Hole 454A									
5-1, 133–136	68.35	1.99×10^{-3}	−11.4	−16.2	135.2	135.4	288[b]	0.380×10^{-3}	14.2
5-2, 102–104	69.53	2.75×10^{-3}	−2.1	−10.3	300.5	309.1	139	1.21×10^{-3}	6.1
5-3, 74–76	70.75	2.79×10^{-3}	+2.0	−11.6	325.5	326.3	130	1.33×10^{-3}	5.7
5-4, 62–64	72.13	3.22×10^{-3}	−1.9	−10.7	156.1	156.6	151	1.23×10^{-3}	7.1
6-2, 110–115	79.13	2.02×10^{-3}	—	—		—	153	1.00×10^{-3}	5.5
8-1, 29–33	95.31	2.74×10^{-3}	—	—		—	566[b]	0.194×10^{-3}	38.7
8-1, 122–125[a]	96.24	0.222×10^{-3}	−17.2	−27.1	217.1	221.9	280	0.293×10^{-3}	2.0
10-1, 51–53	113.52	3.85×10^{-3}	−30.4	−31.4	252.6	255.7	230	0.348×10^{-3}	29.9
11-1, 101–103	123.02	14.1×10^{-3}	−22.4	−35.4	280.0	281.3	157	1.21×10^{-3}	31.5
11-2, 111–113	124.62	11.3×10^{-3}	−38.3	−41.9	152.0	152.8	138	0.987×10^{-3}	30.9
11-3, 91–93	125.92	7.30×10^{-3}	−31.5	−36.4	13.7	12.5	117	1.22×10^{-3}	16.1
11-4, 24–26	126.75	9.86×10^{-3}	−36.1	−38.5	332.9	333.9	118	1.32×10^{-3}	20.2
11-4, 95–97	127.47	5.49×10^{-3}	−31.5	−34.7	49.5	48.9	130	1.15×10^{-3}	12.9
12-1, 112–114	132.13	3.18×10^{-3}	−25.0	−30.4	293.6	296.3	155	0.942×10^{-3}	9.1
12-2, 39–41	132.90	13.6×10^{-3}	−27.7	−29.5	27.0	27.7	141	1.24×10^{-3}	29.6
13-1, 2–4[a]	140.03	14×10^{-6}	+21.6	(−19.2)	323.0	(352.0)	88	0.241×10^{-3}	0.2
13-1, 80–82[a]	140.81	54×10^{-6}	−5.9	−23.0	106.8	119.4	191[b]	0.341×10^{-3}	0.4
14-1, 20–23	149.22	7.22×10^{-3}	—	—	—	—	546[b]	0.228×10^{-3}	85.6
15-1, 4–8	158.06	7.33×10^{-3}	—	—	—	—	376	0.299×10^{-3}	66.3
16-1, 82–84	162.83	4.02×10^{-3}	−15.5	−16.6	257.2	256.9	227	0.376×10^{-3}	28.9
16-2, 14–16	163.65	8.95×10^{-3}	−10.4	−19.6	245.6	245.6	435[b]	0.260×10^{-3}	93.1
Hole 456									
16-1, 20–22	133.71	0.386×10^{-3}	−45.9	−45.9	333.7	334.7	154	0.205×10^{-3}	5.0
16-1, 25–27	133.76	2.99×10^{-3}	−36.1	−44.3	328.1	334.0	95	2.94×10^{-3}	3.1
16-2, 99–101	136.00	5.92×10^{-3}	−26.9	−27.9	180.3	180.4	147	2.37×10^{-3}	7.1
18-1, 53–55	153.04	1.94×10^{-3}	−23.4	−26.6	236.5	240.8	208[b]	0.806×10^{-3}	7.2
Hole 458									
28-1, 90–92	257.41	0.957×10^{-3}	+25.7	+34.4	355.3	354.7	185	1.31×10^{-3}	2.0
29-1, 121–124	267.23	2.21×10^{-3}	+42.0	+37.8	118.5	118.0	211	1.07×10^{-3}	5.6
29-2, 92–94	268.43	0.579×10^{-3}	+30.3	+35.3	345.9	339.8	221	1.13×10^{-3}	1.4
29-3, 64–66	269.65	1.18×10^{-3}	+30.0	+33.1	241.9	238.5	225	1.19×10^{-3}	2.7
30-1, 105–107	276.56	1.51×10^{-3}	+12.1	+13.6	37.8	39.0	261	1.05×10^{-3}	3.9
30-2, 56–58	277.57	1.25×10^{-3}	+16.6	+14.9	145.8	147.0	257	1.16×10^{-3}	2.9
31-1, 121–123	286.22	0.656×10^{-3}	+26.0	+34.5	195.4	192.1	178	1.55×10^{-3}	1.1
32-1, 72–74	295.23	0.630×10^{-3}	+35.0	+34.5	66.8	67.3	197	1.44×10^{-3}	1.2
32-2, 118–120	297.19	0.465×10^{-3}	+27.3	+31.8	107.3	107.7	138	1.49×10^{-3}	0.8
32-3, 119–121	298.70	3.31×10^{-3}	+19.9	+31.3	212.5	212.9	151	1.42×10^{-3}	6.3
33-1, 115–117	305.16	0.708×10^{-3}	+20.1	+35.9	221.8	226.3	228[b]	1.70×10^{-3}	1.1
33-2, 42–44	305.93	0.988×10^{-3}	+28.0	+34.0	95.5	96.9	252	1.45×10^{-3}	1.8
34-1, 123–125	314.74	1.83×10^{-3}	+28.3	+29.9	83.8	82.1	168	1.32×10^{-3}	3.8

Table 2. (Continued).

Sample (interval in cm)	Depth below Sea Floor (m)	J_{NRM} (emu/cm^3)	I_{NRM}	I_{Stable}	D_{NRM}	D_{Stable}	MDF (Oe)	k	Q
Hole 458									
34-2, 30-32	315.31	0.479×10^{-3}	+29.4	+34.7	107.5	109.2	204	1.22×10^{-3}	1.1
35-1, 97-99	323.98	0.183×10^{-3}	+56.2	+58.2	64.0	49.7	152[b]	1.15×10^{-3}	0.4
35-1, 103-105	324.04	0.468×10^{-3}	+30.1	+28.4	42.0	36.8	189[b]	1.24×10^{-3}	1.0
35-1, 133-135	324.34	0.313×10^{-3}	+13.8	+7.5	329.0	318.7	179[b]	1.19×10^{-3}	0.7
35-1, 137-139	324.38	0.892×10^{-3}	+35.8	+34.5	8.0	7.0	183[b]	1.23×10^{-3}	2.0
35-2, 46-48	324.97	2.12×10^{-3}	+25.7	+28.2	88.2	87.3	242	1.27×10^{-3}	4.5
36-1, 55-57	333.06	1.59×10^{-3}	+37.2	+32.5	104.3	104.9	280	0.892×10^{-3}	4.8
36-2, 22-24	334.23	0.799×10^{-3}	+18.2	+18.4	52.0	53.5	310	0.682×10^{-3}	3.2
37-1, 142-144	343.43	3.36×10^{-3}	+21.0	+23.3	239.8	238.2	183	1.28×10^{-3}	7.1
37-2, 77-79	344.28	5.64×10^{-3}	+29.1	+21.0	90.9	90.3	279	1.33×10^{-3}	11.5
38-1, 55-57	352.06	0.894×10^{-3}	+18.6	+19.3	244.8	245.9	169	1.51×10^{-3}	1.6
39-1, 106-108	362.07	1.17×10^{-3}	+37.3	+37.5	227.8	228.4	306	0.907×10^{-3}	3.5
39-2, 51-53	363.02	0.776×10^{-3}	+33.8	+35.1	337.4	335.0	268	0.877×10^{-3}	2.4
39-3, 15-17	364.16	0.529×10^{-3}	+35.6	+35.7	193.0	193.8	253	1.07×10^{-3}	1.3
40-1, 134-137	371.86	1.34×10^{-3}	+33.5	+34.7	181.5	180.9	264	1.02×10^{-3}	3.6
40-2, 72-75	372.74	1.64×10^{-3}	+45.7	+38.0	132.9	132.3	364	0.723×10^{-3}	6.1
40-2, 115-117	373.16	1.07×10^{-3}	+42.1	+40.2	89.8	91.3	361	0.676×10^{-3}	4.3
41-1, 3-5	380.04	2.68×10^{-3}	−16.1	−15.6	11.2	13.0	213	1.77×10^{-3}	4.1
43-1, 146-148	400.47	1.14×10^{-3}	−6.6	−9.3	344.8	355.7	180	1.45×10^{-3}	2.1
43-2, 19-21	400.70	1.36×10^{-3}	−10.5	−9.7	97.2	88.3	175	1.60×10^{-3}	2.3
44-1, 6-8	408.57	2.00×10^{-3}	−11.4	−12.3	105.1	96.4	186	1.64×10^{-3}	3.3
44-1, 37-39	408.88	1.06×10^{-3}	−12.6	−13.2	345.3	346.4	550[b]	0.267×10^{-3}	10.7
45-1, 117-119	419.18	1.84×10^{-3}	−3.8	−4.0	352.7	352.5	230	1.47×10^{-3}	3.4
45-2, 29-31	419.80	0.918×10^{-3}	−2.7	−5.6	181.4	179.1	151	1.40×10^{-3}	1.8
46-1, 88-90	428.39	25.7×10^{-3}	−3.6	−4.2	346.5	346.8	165	2.27×10^{-3}	30.6
47-1, 36-38	437.37	10.7×10^{-3}	−10.4	−10.5	44.8	42.4	151	2.53×10^{-3}	11.4
Hole 459B									
60-1, 121-124	560.13	4.11×10^{-3}	+27.9	+13.4	8.6	2.8	109[b]	1.52×10^{-3}	7.3
60-2, 61-63	561.02	32.0×10^{-3}	+10.0	+11.4	122.0	122.4	90	1.70×10^{-3}	50.8
61-1, 85-87	568.86	0.535×10^{-3}	−2.9	−8.7	113.8	89.3	87	1.36×10^{-3}	1.1
61-1, 140-142	569.41	9.60×10^{-3}	−7.2	−10.3	337.6	338.4	90	1.68×10^{-3}	15.4
61-2, 81-82	570.32	0.721×10^{-3}	−15.8	−15.4	343.0	345.0	123[b]	1.28×10^{-3}	1.5
62-1, 47-49	577.98	1.24×10^{-3}	−25.6	−14.5	35.0	18.3	139	1.46×10^{-3}	2.3
63-1, 49-51	587.50	20.1×10^{-3}	+10.4	+11.7	158.0	158.0	157	1.52×10^{-3}	35.7
64-1, 23-25	596.74	35.6×10^{-3}	−25.4	−23.6	68.4	68.6	116	1.76×10^{-3}	54.7
65-1, 83-85	606.84	42.0×10^{-3}	+44.1	+45.0	16.5	16.4	147	2.29×10^{-3}	49.6
66-1, 39-41	615.90	6×10^{-6}	+15.3	(+11.1)	346.1	(113.1)	—	2.87×10^{-3}	10^{-2}
66-2, 137-139	618.38	0.860×10^{-3}	+0.2	(+11.1)	199.1	(84.3)	62	3.79×10^{-3}	0.6
67-1, 134-136	626.35	0.645×10^{-3}	+23.8	+11.0	355.8	1.5	188[b]	2.18×10^{-3}	0.8
67-2, 71-73	627.22	0.983×10^{-3}	+10.8	+9.8	237.9	251.1	128	2.81×10^{-3}	1.0
68-1, 33-35	634.84	0.733×10^{-3}	+12.1	+12.9	148.0	154.4	162	1.90×10^{-3}	1.0
69-1, 44-46	644.45	2.05×10^{-3}	+14.3	+12.4	283.1	286.9	218	1.57×10^{-3}	3.5
69-2, 125-127	646.76	1.20×10^{-3}	−19.0	−12.2	318.6	330.0	307	1.66×10^{-3}	2.0
69-3, 79-81	647.80	13.2×10^{-3}	−4.3	−8.9	147.5	141.7	132	2.28×10^{-3}	15.7
70-1, 46-48	653.97	3.81×10^{-3}	−2.5	−3.4	4.1	0.0	196	1.87×10^{-3}	5.5
71-1, 39-41	663.40	3.31×10^{-3}	+13.4	+6.1	187.0	184.3	182	3.15×10^{-3}	2.8
71-1, 130-132	664.31	6.92×10^{-3}	+3.6	+5.3	189.9	185.7	182	2.32×10^{-3}	8.1
71-2, 30-32	664.81	5.82×10^{-3}	+4.4	+4.6	235.2	236.9	161	2.48×10^{-3}	6.3
72-1, 54-56	673.05	11.1×10^{-3}	+3.3	+4.9	232.1	233.4	135	2.50×10^{-3}	12.0
72-1, 134-136	673.85	66.3×10^{-3}	+13.8	+12.6	91.9	90.6	144	2.40×10^{-3}	74.4
73-1, 25-27	682.26	11.2×10^{-3}	+1.7	+4.8	57.0	50.6	158	2.46×10^{-3}	12.3
73-2, 139-141	684.90	22.0×10^{-3}	+2.8	+3.8	282.8	284.4	143	2.30×10^{-3}	25.9
73-3, 28-30	685.29	7.33×10^{-3}	+12.0	+13.5	322.3	323.7	180	1.90×10^{-3}	10.4

Notes:

I_{NRM}, D_{NRM} = directions of natural remanent magnetization; I = inclination in degrees with respect to horizontal, negative above horizon; D = declination in degrees with reference to an arbitrary zero azimuth.

I_{Stable}, D_{Stable} = stable magnetization direction as resulting from an AF or thermal demagnetization analysis, brackets indicate a limited degree of reliability;

MDF = median destructive field in Oe; for Hole 453 underlined values give MDT (median destructive temperature) in °C as resulting from a thermal demagnetization treatment.

k = initial susceptibility in emu/cm^3 • Oe.

Q = Königsberger ratio, present ambient field F = 0.37 Oe.

[a] Sediments.

[b] Denotes the presence of spurious magnetization components.

Table 3. Lithologic and paleomagnetic units, Leg 60.

Lithologic Units (intervals in m)	Paleomagnetic Units (intervals in m)	I_{Stable}
Hole 453		
I 455.50–541.00	I 465.41–500.72	−9.4 ± 1.4
	II 466.92–506.07	+23.6 ± 1.0
	III 496.80–535.62	+56.8 ± 4.6
	IV 498.07–536.61	−48.4 ± 2.5
II 541.00–569.50	(no oriented samples)	—
III 569.50–605.00	(no oriented samples)	—
"no-magnetization" zone: 518.42–523.88		
Hole 454A		
67.00–76.50	I 68.35–72.13	I −12.2 ± 2.7
II 78.90–86.00	(no oriented samples)	—
III 86.00–96.00	(no oriented samples)	—
and 104.00–119.00	II (one sample)	−31.4
IV 119.00–129.00	III 123.02–127.47	−37.4 ± 2.9
and 131.00–140.00	IV 132.13–132.90	−30.0 ± 0.6
V 149.00–171.50	V 162.83–163.65	−18.1 ± 2.1
Hole 456		
I 133.50 – 152.50	I 133.71–133.76	−44.7 ± 0.5
	II 136.00–153.04	−27.3 ± 0.9
III 152.50–169.00	(no oriented samples)	
Hole 458		
I 256.50–286.10	I 257.41–269.65	+35.2 ± 2.0
	II 276.56–277.57	+14.3 ± 0.9
II 286.10–351.50	III 286.22–333.06	+32.5 ± 2.6
	IV 334.23–352.06	+20.5 ± 2.2
III 351.50–380.00	V 362.07–373.16	+36.9 ± 2.1
IV 380.00–428.10	VI 380.04–408.88	−12.0 ± 2.6
	VII 419.18–428.39	−3.4 ± 0.6
V 428.10–465.50	VIII 437.37–? (one sample)	−10.4
Hole 459B		
I 558.90–587.00	I 560.13–561.02	+12.4 ± 1.4
	II 568.86–577.98	−12.2 ± 3.2

Table 3. (Continued).

Lithologic Units (intervals in m)	Paleomagnetic Units (intervals in m)	I_{Stable}
Hole 459B		
II 587.00–615.50	III (one sample)	+11.7
	IV (one sample)	−23.6
III 615.50–644.00	V 615.90–644.45	+11.4 ± 1.1
IV 644.00–691.50	VI 646.76–653.97	−8.2 ± 4.5
	VII 663.40–685.29	+7.0 ± 3.8

Note: Dashed lines indicate that boundary is not in complete agreement.